University of Maribor
Faculty of Energy Technology

Journal of ENERGY TECHNOLOGY

Volume 16 / Issue 4
DECEMBER 2023
www.fe.um.si/en/jet.html

Journal of ENERGY TECHNOLOGY

VOLUME 16 / Issue 4

Revija Journal of Energy Technology (JET) je indeksirana v bazah INSPEC© in Proquest's Technology Research Database.

The Journal of Energy Technology (JET) is indexed and abstracted in database INSPEC© and Proquest's Technology Research Database.

JOURNAL OF ENERGY TECHNOLOGY

Ustanovitelj / FOUNDER

Fakulteta za energetiko, UNIVERZA V MARIBORU /
FACULTY OF ENERGY TECHNOLOGY, UNIVERSITY OF MARIBOR

Izdajatelj / PUBLISHER

Fakulteta za energetiko, UNIVERZA V MARIBORU /
FACULTY OF ENERGY TECHNOLOGY, UNIVERSITY OF MARIBOR

Tehnični urednik / TECHNICAL EDITOR

Sonja KRAJNC

Tehnična podpora / TECHNICAL SUPPORT

Tamara BREČKO BOGOVČIČ

Izhajanje revije / PUBLISHING

Revija izhaja štirikrat letno v nakladi 100 izvodov. Članki so dostopni na spletni strani revije - www.fe.um.si/si/jet.html / The journal is published four times a year. Articles are available at the journal's home page - www.fe.um.si/en/jet.html.

Cena posameznega izvoda revije (brez DDV) / Price per issue (VAT not included in price): 50,00 EUR.

Informacije o naročninah / Subscription information:
http://www.fe.um.si/en/jet/subscriptions.html

Lektoriranje / LANGUAGE EDITING

Shelagh MARGARET HEDGES (EN), AMIDAS d.o.o. (SLO)

Oblikovanje in tisk / DESIGN AND PRINT

Tiskarna Saje d.o.o.

Naslovna fotografija / COVER PHOTOGRAPH

Jurij AVSEC

Oblikovanje znaka revije / JOURNAL AND LOGO DESIGN

Andrej PREDIN

Ustanovni urednik / FOUNDING EDITOR

Andrej PREDIN

Izdajanje revije JET finančno podpira Javna agencija za raziskovalno dejavnost Republike Slovenije iz sredstev državnega proračuna iz naslova razpisa za sofinanciranje domačih znanstvenih periodičnih publikacij / The Journal of Energy Technology is co-financed by the Slovenian Research Agency.

Spoštovani bralci revije Journal of energy technology (JET)

Vse od začetkov človeštva so bili ogrevanje bivališč, kurjenje in toplotna obdelava hrane izjemnega pomena. Tudi v današnjem času človeštvo porabi velik del energije za ogrevanje in hlajenje. Čeprav so sistemi ogrevanja zelo napredovali in se je močno izboljšal izkoristek naprav, ljudje še vedno porabimo približno 50 % vse energije za ogrevanje. Ogrevanje v svetu še vedno večinoma poteka s pomočjo fosilnih goriv. Približno polovica energije se porabi za industrijsko ogrevanje, preostala polovica pa za ogrevanje stavb, sanitarne vode, kuhanje in potrebe po toploti v kmetijstvu. Večino toplotne energije še vedno pridobimo s pomočjo zgorevanja fosilnih goriv. Procesi ogrevanja prispevajo približno 40 % vseh emisij ogljikovega dioksida.

Glede na svetovno ekološko situacijo mislim, da je skrajni čas za intenzivno uporabo obnovljivih virov v mnogo večji meri. Tudi procesi soproizvodnje toplote in električne energije ter uporabe toplotnih črpalk bi morali prispevati k precejšnjemu zmanjšanju emisij toplogrednih plinov. Z intenzivno uporabo vodikovih tehnologij bi lahko veliko prispevali tudi k izboljšanju ekološke situacije …

Vsem bralcem želim zanimivo branje nove številke revije JET in upam, da bo vsak našel kaj zanimivega.

Jurij AVSEC
odgovorni urednik revije JET

Dear Readers of the Journal of Energy Technology (JET)

Since the beginning of mankind the heating of dwellings, burning and thermal processing of food have been of the utmost importance. Even today, humanity uses a large part of energy for heating and cooling. Despite the fact that heating systems have advanced greatly, and the efficiency of devices has improved greatly, people still use approximately 50% of all energy for heating in the world. Heating in the world is still done mainly with the help of fossil fuels. About half of the energy is used for industrial heating, and the remaining half for heating buildings, sanitary water, cooking and heat needs in agriculture. The majority of thermal energy is still obtained by burning fossil fuels. Heating processes contribute about 40% of all carbon dioxide emissions.

Considering the global ecological situation, I think that the time has come for the intensive use of renewable resources to a much greater extent. The processes of co-production of heat and electricity and the use of heat pumps should also contribute to a substantial reduction of greenhouse gas emissions. Furthermore, with the intensive use of hydrogen technologies, we could make a substantial contribution to improving the ecological situation...

I wish all readers an interesting reading of the new issue of JET magazine, and I hope that everyone will find something interesting .

Jurij AVSEC
Editor-in-chief of JET

Table of Contents
Kazalo

Journal of Energy Technology

JET Volume 16 (2023) p.p. 11-17
Issue 4, 2023
Type of article: 1.01
http://www.fe.um.si/si/jet.htm

ANALYTICAL ESTIMATION OF THE THERMAL STABILITY OF HTS MAGNETS DURING SUDDEN DISCHARGE

ANALITIČNA OCENA TOPLOTNE STABILNOSTI HTS-MAGNETOV MED NENADNIM PRAZNENJEM

Takanobu Mato[✉], **So Noguchi**[2]

Keywords: HTS magnets, no-insulation technique, thermal stability, analytical expression

Abstract

Since the advent of 2nd-generation high-temperature superconducting (HTS) tapes, which show great features on critical temperature, critical current density, and critical magnetic field, many researchers have been trying to generate ultra-high magnetic fields using HTS coils. One more promising technology is a no-insulation (NI) winding technique. This technique suppresses the possibility of thermal runaway and burning-out of HTS coils drastically. The interest in compact nuclear fusion magnets wound with HTS conductors has been increasing rapidly during the last five years. The simulation of such magnets larger than MRI/NMR HTS magnets takes an unfeasibly long time. Therefore, we present a simple expression of the coil temperature rise under a simple assumption derived from the simple coil model, to investigate the stability of large-scale magnets.

The method's advantages are simplicity, versatility, and nearly no computation, enabling a time reduction in the first-cut design.

Povzetek

Od pojava superprevodnih trakov druge generacije, ki delujejo pri visokih temperaturah (HTS) in ki izkazujejo izjemne značilnosti v smislu kritične temperature, gostote kritičnega toka in kritičnega magnetnega polja, si številni raziskovalci prizadevajo za generiranje ultravisokih magnetnih polj

✉ Corresponding author: Mr. Takanobu Mato, Hokkaido University, Information Science and Technology, Kita 14, Nishi 9, Kita-ku, Sapporo, Hokkaido, 060-0814, Japan, Tel.: +81-11-706-7670, E-mail address: mato@em.ist.hokudai.ac.jp

2 Hokkaido University, Department, Information Science and Technology, Kita 14, Nishi 9, Kita-ku, Sapporo, Hokkaido, 060-0814, Japan

z uporabo HTS-tuljav. Obetavna tehnologija na tem področju je tehnika navijanja brez izolacije (NI). Ta pristop znatno zmanjša tveganje za termični preboj in izgorevanje HTS-tuljav. V zadnjih petih letih opažamo večje zanimanje za kompaktne magnete jedrske fuzije, ki so naviti s HTS-prevodniki. Simulacija takih magnetov, večjih od HTS-magnetov, uporabljenih v MRI-/NMR-napravah, zahteva neizvedljivo dolg čas. Zato v tem članku predstavljamo preprost izraz za opis dviga temperature tuljave, ki temelji na preprosti predpostavki, izpeljani iz osnovnega modela tuljave, s ciljem raziskovanja stabilnosti magnetov velikih dimenzij. Glavne prednosti predlagane metode so njena preprostost, univerzalnost in minimalna potreba po računskih operacijah, kar omogoča skrajšanje časa začetnega načrtovanja.

1 INTRODUCTION

Towards the future of nuclear fusion power, our group is trying to establish a way to simulate and evaluate the thermal stability of superconducting magnets to generate ultra-high magnetic fields. Superconducting magnets wound with high-temperature superconductors (HTS), especially Rare-Earth Barium Copper Oxide (REBCO) [1], are considerably promising for the magnetic confinement of plasma. HTS tapes, such as REBCO-coated conductors, can maintain superconductivity in high magnetic fields (> 20 T). In 2011, Hahn et al. proposed a no-insulation (NI) winding technique for HTS pancake coils [2], where there is no insulation between the winding turns. The NI winding technique improves the thermal stability of HTS pancake coils greatly, solving the long-lasting thermal instability for high magnetic field generation [3], [4]. The mechanism of the high thermal stability is explained as follows [5]: a hot spot, which potentially causes a thermal runaway, appears in an NI HTS coil. The operating current can flow into the adjacent turns through the turn-to-turn contact surfaces, avoiding the hot spot. The consequent Joule heat dissipation is less than the case of a conventionally turn-insulated HTS coil.

As a matter of fact, a metal-insulation winding technique, which is categorized as one of the no-insulation winding techniques, was adopted to generate 20 T for a nuclear fusion coil at MIT [6]. The electromagnetic, thermal, and mechanical behaviors of NI HTS coils are complicated, and the simulation takes a long time, even to evaluate the thermal stability [7]. Furthermore, a fine simulation of such a large-scale NI HTS magnet is complex. Several researches and developments have been made on NI HTS magnet simulation methods; however, a fast and easy way to evaluate thermal stability is still necessary as a fundamental step of thermal stability designs.

This paper proposes a simple analytical expression of NI HTS coil temperature. It is useful in the first-cut conceptual design. The formulation is given in the paper, and an arbitrary NI REBCO coil was investigated with different parameters. The maximum temperatures reached were checked as a function of the radial turn-to-turn resistance. For such a large magnet, a cooling effect is not negligible due to the long time constant. The timescale of heat dissipation and cooling effect is also discussed in the paper. The proposed expression for thermal evaluation enables the parameter survey as well. This helps clarify the thermal stability boundary, which will be addressed in the future.

2 MODEL AND FORMULATION

2.1 Circuit Model

Fig. 1 shows an electrically equivalent circuit of an NI HTS magnet. The NI HTS coils are stacked and connected in series, forming the NI HTS magnet. The NI HTS magnet has the self-inductance L.

The introduction mentions that each NI HTS coil has a radial current path through the turn-to-turn contact surfaces. The resistance in the radial direction is expressed as a radial resistance R_r connected in parallel with the magnet inductance L. The current source is not shown in the equivalent circuit, because only the cases of sudden discharge tests are evaluated (mentioned later).

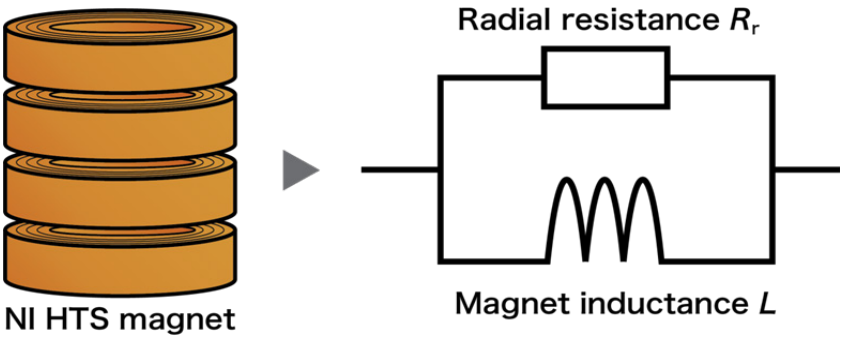

Figure 1: *Electrically equivalent circuit of an NI HTS magnet*

2.2 Formulation of Coil Temperature

From the above-shown electrically equivalent circuit model, we derived the current and temperature of the NI HTS magnet, considering the cooling effect. Here, the NI HTS magnet was assumed to be disconnected from a power source as the worst scenario, commonly called a sudden discharge test. The magnet is immersed in a coolant such as liquid helium. The magnet current I during discharging decays exponentially; the following Equation expresses it:

$$I = I_m e^{-\frac{t}{\tau_e}} \tag{2.1}$$

where I_m and t are the initial operating current and the time, respectively. It is noted that τ_e is the magnet time constant defined by

$$\tau_e = \frac{L}{R_r} \tag{2.2}$$

Using Equation (2.1), the magnet temperature T is governed by the Equation below:

$$C\frac{dT(t)}{dt} = R_r I^2 - H\{T(t) - T_i\} \tag{2.3}$$

Here, C, H, and T_i are the magnet thermal capacity [J/K], the thermal transfer coefficient [W/K], and the initial magnet temperature [K], respectively. Now, solving Equation (2.3), and the analytical expression of temperature T after disconnection of the power source is derived as follows:

$$T(t) = \frac{LI_m^2}{H\tau_e - 2C}\left(e^{-\frac{2t}{\tau_e}} - e^{-\frac{t}{\tau_t}}\right) \tag{2.4}$$

where τ_t is the thermal time constant, and it is calculated by

$$\tau_t = \frac{C}{H} \tag{2.5}$$

3 ANALYTICAL RESULTS

The current and temperature transitions of large-scale NI HTS magnets were investigated in this Section. Table 1 shows the magnet specifications. The magnet generates approximately 10 T at the magnet center. It was assumed that the magnet was immersed in liquid helium, and the heat could only move through the magnet surfaces in contact with the liquid helium. The heat is transferred according to Newton's law of cooling. The heat transfer coefficient was also assumed constant at 100 W/(m^2·K) [8].

The current profiles after the power shutdown at t = 0 s are shown in Fig. 2 in the cases of radial resistances 10, 50, and 100 μΩ as a design parameter. The magnet current decays exponentially, and the time constant shortens as the high radial resistance. The magnet is heated with the Joule heat by the current passing through the radial current.

Fig. 3 shows the magnet temperature in the three cases of different radial resistances. The temperature increases rapidly, and reaches a maximum after the power shutdown due to the cooling. In the case of radial resistance 100 μΩ, the maximum temperature is 172 K. It is noted that the lower the resistance is, the lower is the reached maximum temperature. This is because a low resistance results in a long time constant, i.e., a long time for energy dissipation and sufficient cooling.

Table 1: *Magnet specifications*

Parameter	Value
inner diameter [m]	0.50
outer diameter [m]	1.0
height [m]	0.3
magnet inductance [mH]	70
mass density [kg/m3]	9000
specific heat [J/(kg·K)]	100
heat transfer coefficient [W/(m2·K)]	100
magnetic energy [MJ]	56
initial current [kA]	40
operating temperature [K]	4.2

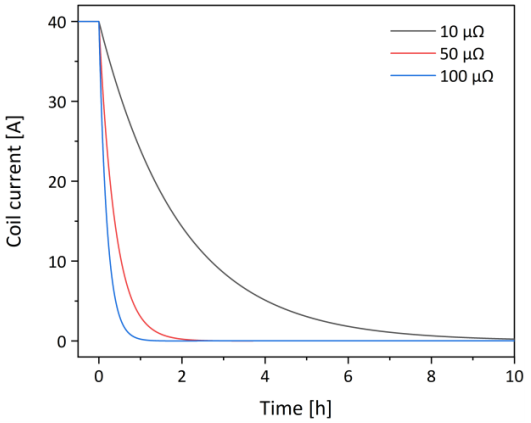

Figure 2: *Coil current of an NI HTS coil with different radial resistance by Equation (2.1)*

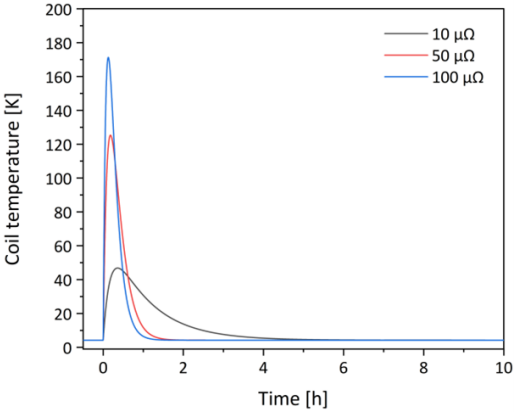

Figure 3: *Temperature of an NI HTS coil with different radial resistance by Equation (2.4)*

Next, the maximum reached temperatures were investigated as a function of the radial resistances. The result is shown in Fig. 4. The maximum temperature increased monotonically and saturated at ~352 K. In the thermal stability view of NI HTS magnets, the increased temperature should be within 300 K to prevent coil performance degradation [8]. The reference line is also drawn in the Figure. When the radial resistance is beyond 1 mΩ, the increased temperature exceeds 300 K. The electrical time constant τ_e is also shown in Fig. 4. It is evident that the low resistance led to the long electrical time constant, and the consequent temperature rise was low.

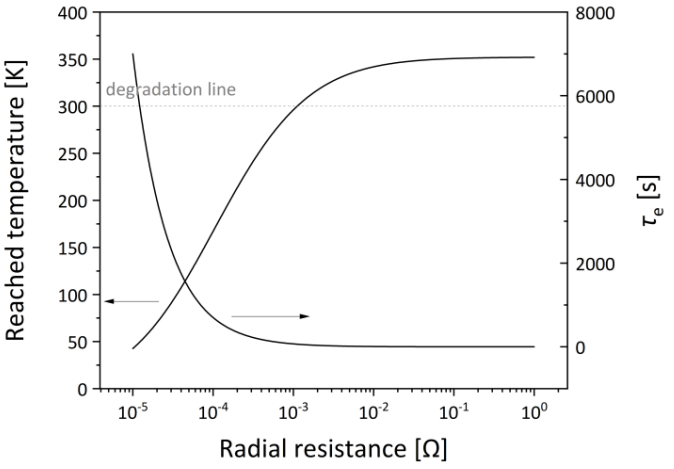

Figure 4: *Reached temperature of HTS magnet as a function of radial resistance*

It is shown that the balance of the timescale of energy dissipation and cooling affects the thermal stability significantly . Now, we introduced the ratio of the electrical time constant to the thermal time constant, α, as below:

$$\alpha = \frac{\tau_t}{\tau_e} \tag{3.1}$$

The ratio computed as a function of the radial resistance is shown in Fig. 5. Here, it is noted that the thermal time constant τ_t remained constant at 614 s. The ratio increased linearly as the electrical time constant τ_e decreased. The high ratio α means the heat dissipation occurred within a short time so as not to cool the magnet effectively. It is shown that the ratio α is one at around 0.1 mΩ. Whereas the ratio α is ~100 at 10 mΩ; i.e., the cooling effect is 1/100 times better from the viewpoint of Joule heat dissipation. Around the region of α = 100, the reached maximum temperature is fully saturated in Fig. 4. In such a large-scale NI REBCO magnet with a long time constant, the radial resistance plays a significant role in thermal stability, and must be designed meticulously.

4 CONCLUSIONS

In the paper, we have proposed the simple stability-evaluation expression of no-insulation (NI) high-temperature superconducting (HTS) magnets. The formulation is shown of the magnet temperature during sudden discharging. It can be used to evaluate the thermal stability of large-scale NI HTS magnets. Several parameter surveys were also conducted using the proposed formula. The results showed that the radial resistance should be low to suppress the high temperature rise by enabling long Joule heat dissipation, whereas the time constant is long. Optimizing the radial resistance is needed [9], [10]. Further analysis is ongoing using the proposed formula.

References

[1] M. Wu ***et al***.: *Superconductivity at 93 K in a new mixed-phase Yb-Ba-Cu-O compound system at ambient pressure,* Phys. Rev. Lett, Vol. 5, Iss. 9, p.p. 908-910, 1987

[2] **S. Hahn *et al*.:** *HTS pancake coils without turn-to-turn insulation,* IEEE Trans. Appl. Supercond, Vol. 21, Iss. 3, p.p. 1592-1595, 2011

[3] **S. Hahn *et al*.:** *45.5-Tesla direct-current magnetic field generated with a high-temperature superconducting magnet,* nature, Vol. 570, p.p. 496-499, 2019

[4] **J. Llu *et al*.:** *World record 32.35-tesla direct-current magnetic field generated with whole superconductor magnet,* Supercond. Sci. Technol, Vol. 33, Iss. 3, Art. no. 03LT01, 2020

[5] **A. Ikeda *et al*.:** *Transient behaviors of no-insulation REBCO pancake coil during local normal-state transition,* IEEE Trans. Appl. Supercond, Vol. 26, Iss. 4, 2016

[6] **D. Chandler *et al*.:** *MIT-designed project achieves major advance toward fusion energy,* MIT news, available at https://news.mit.edu/2021/MIT-CFS-major-advance-toward-fusion-energy-0908, 2021

[7] **S. Noguchi *et al*.:** *A newly developed screening current simulation method for REBCO pancake coils based on extension of PEEC model,* Supercond. Sci. Technol, Vol. 35, Iss. 4, Art. no. 04400, 2020

[8] **Y. Iwasa *et al*.:** *Case studies in superconducting magnets: design and operational issues,* Springer: New York, 2009

[9] **Y. Suetomi *et al*.:** *Quench and self-protecting behavior of an intra-layer no-insulation (LNI) REBCO coil at 31.4 T,* Supercond. Sci. Technol, Vol. 34, Iss. 6, Art. no. 064003, 2021

[10] **S. Noguchi *et al*.:** *A simple protection evaluation method for no-insulation REBCO pancake coils during local normal-state transition,* Supercond. Sci. Technol, Vol. 32, Iss. 4, Art. no. 045001, 2019

Journal of Energy Technology

JET Volume 16 (2023) p.p. 18-28
Issue 4, 2023
Type of article: 1.01
http://www.fe.um.si/si/jet.htm

CHARGING STATIONS CONNECTED TO STREET LIGHT POWER SYSTEMS

POLNILNE POSTAJE PRIKLJUČENE NA ELEKTROENERGETSKI SISTEM ULIČNE RAZSVETLJAVE

Peter Janiga[R]

Keywords: street lighting, public lighting, charger, charging station, power quality, electric vehicle, lamp, luminaire

Abstract

Street light grids are dense and compact networks in all cities. They power the luminaires and elements of smart cities. Recently, they have also been used to power chargers for electric vehicles. The article analyses how charging stations can be connected to public lighting networks, and gives knowledge about connecting the charger and optimising operations to increase the power delivered to vehicles. Initial installations show that the combination of luminaires, public lighting networks and chargers shows specific characteristics. The aim of the paper is to provide knowledge about the implementation of chargers in street light grids. The last part of the paper presents the results a case study, which is focused on voltage drops and limits for installing charging stations.

Povzetek

Elektroenergetski sistemi za ulično razsvetljavo so gosta in kompaktna omrežja v vseh mestih. Napajajo svetila in elemente pametnih mest. V zadnjem času se uporabljajo tudi za napajanje polnilnic električnih vozil. Članek analizira, kako lahko polnilne postaje priključimo na omrežja javne razsvetljave, podaja znanja o priklopu polnilnika in optimizaciji delovanja za povečanje moči, ki se pretaka v vozila. Začetne inštalacije kažejo, da kombinacija svetilk, omrežij javne razsvetljave

[R] Corresponding author: Assoc. Prof., Peter Janiga, Slovak University of Technology in Bratislava, Faculty of Electrical Engineering and Information Technology, Ilkovičova 3, 84104 Bratislava, Tel.: +421 2 6029 1811, E-mail address: peter.janiga@stuba.sk

in polnilnic kaže specifične značilnosti. Namen prispevka je podati znanje o implementaciji polnilnic v omrežja javne razsvetljave. Zadnji del prispevka predstavlja rezultate študije primera, ki se osredotoča na padce napetosti in omejitev za namestitev polnilnih postaj.

1 INTRODUCTION

Street light grids (SLG) are the main parts of cities and municipalities. They are on all the streets. They are a network that covers the entire city and allows smart city elements to be powered. A specific feature of an SLG is that the main appliance (luminaire) is switched on only at night. These properties create possibilities for the use of SLG to power charging stations for electric vehicles. There are already several projects in the world, but there is not enough experience and information on how to build and operate these common networks [9].
Charging modes

In relation to the method of connecting the vehicle to the power network, the EN 61851-1 [1] Standard defines four possible connection modes.

- Mode 1 - In this case, a standardised socket with a nominal current value not exceeding 16A is used to connect to the AC supply voltage network. It can be a single-phase socket with a nominal voltage of 230V, or a three-phase socket with a nominal voltage of 400V, in both cases with a protective earth conductor.
- Mode 2 - In this case, a standardised socket with a rated current value not exceeding 32A is used to connect to the AC supply voltage network. It can be a single-phase socket with a nominal voltage of 230V, or a three-phase socket with a nominal voltage of 400V, in both cases with a protective earth conductor. The difference from mode 1, in addition to the rated current, is the need to use a charge control circuit with separate electrical protection in this case. The circuit is integrated directly into the control box of the charging cable, which must be at a distance of 0.3m from the plug, or directly on it.
- Mode 3 - Is charging through a device reserved only for charging electric vehicles. The device is connected permanently to the AC power supply. It is necessary to use a charging control circuit that communicates with the device (charging station) during the entire charging period.
- Mode 4 - In the first three modes charging was carried out using the vehicle's on-board charger. The fourth mode uses a charger located outside the vehicle's deck to connect the vehicle to the power network. The charger can be powered from an AC or DC network. However, the standard is to be powered by an AC current, which must be converted to a DC current in a charging station outside the vehicle. Even in this case, communication is necessary, where the charging control circuit communicates with the public charging station during the entire charging period.

The method of charging electric vehicles and their integration into the distribution grid can have a significant impact on the energy system. In the case of high-power charging at fast-charging stations with high capacity, managing substantial amounts of electrical energy simultaneously may necessitate adjustments in the distribution grid. Peak load management is crucial, as the current collective surge in charging can create peak loads on the grid. Implementing an intelligent charging infrastructure that can optimise charging based on the current state of the grid is essential. The development of technologies and strategies for electric vehicle charging plays a crucial role in the pursuit of a sustainable and efficient integration into the energy system.

2 METHODS

The calculation methodology is based on the definition of boundary conditions such as operating charging stations in general and existing public lighting networks. The charging stations are divided into AC and DC. This division determines the output power of the charger. Charging stations with an AC current are typically slower than DC stations [8]. Charging with an AC current can be divided into two groups: slow charging with a power of up to 3.7kW, and accelerated charging with a power of 3.7kW to 22kW. When charging with a DC current, we are talking about fast and ultra-fast charging. Fast DC charging is considered to be charging with a power of up to 100kW, while the power of fast charging stations is usually not less than 50kW. Ultra-fast DC charging is charging with a power of more than 100kW.

2.1 Connecting the stations to the street light grids

Although the implementation of charging stations in the SLG is a relatively new topic, there are already several ways to connect and control the station [2]. However, everything depends on the possibilities and current capacity reserves of the SLG, because public lighting is always a primary functionality that cannot be influenced negatively by other additional appliances.

2.2 Implementation of a charging station on a pole

Connecting the charging station to a public lighting pole can be done in two ways. The first of them is the connection of a charging station in the form of a wall box to an existing pole. The second is the integration of the charging station directly into the public lighting pole. This solution is better for networks with reconstructed poles, where it is expected to replace the original poles with new ones. This solution is not visually disturbing, and the public lighting pole looks the same as ordinary poles, except that it contains a charging connector. The third solution is to place the charging station in a separate column. This solution is suitable if there is no pole near or for parking spaces. However, there must be a public lighting cable nearby to power the charging station. From the point of view of installation, this solution is suitable for more extensive renovations, where cable lines are also replaced.

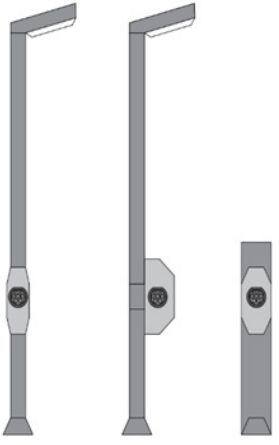

Figure 1: *Charging station integrated to the pole (right), charging station in the form of a wall box (middle), charging station in a separate column*

In all cases, as with all public AC charging stations, the Type 2 connectors defined in EN 61851-1 are used as standard.

2.3 Electrical connection of the charging station

From the point of view of connecting the power line, there are several ways to implement charging stations in the SLG.

The first of them is the connection of the charging station to the power line that is common to public lighting. In this case, intelligent control is necessary, that corrects the maximum power of the charging station based on the current state of the network, so as not to limit the public lighting function. Depending on the possibilities of the network, different capacities of charging stations can be used, up to charging stations with a power of 22kW when supplied from three phases.

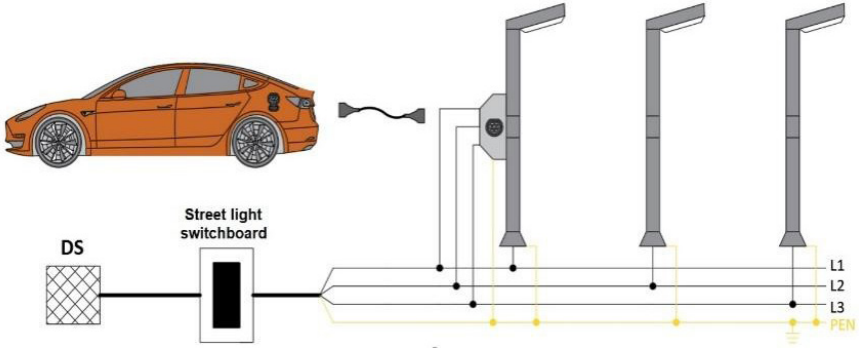

Figure 2: *Connection of the charging station to the power line common with the power supply of the SLG*

The second option is to connect the charging station to only one phase of the three-phase system. This phase is reserved for the power supply of the charger and other appliances (e.g. smart city appliances). In this case, public lighting luminaires are powered from the remaining two phases of the three-phase system. A disadvantage with this connection is the unbalanced load on the phase system and a lower charging power for the user, which is around 7kW (for 230 V).

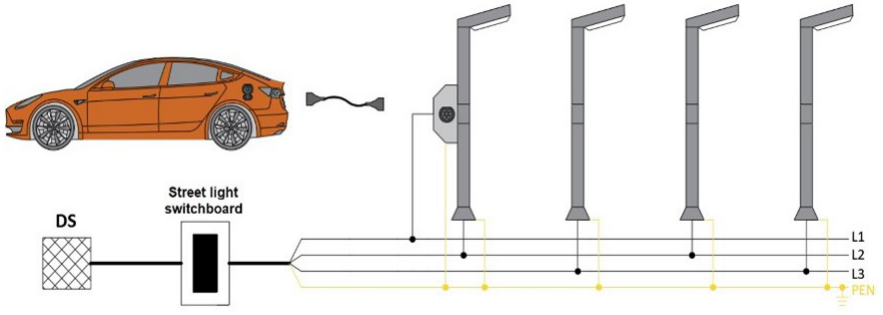

Figure 3: *Connecting the charging station to the reserved one phase of the three-phase system*

Another option is the use of two independent three-phase power lines. One is used exclusively to power the public lighting network, and the other to power charging stations or other additional appliances. This method is advantageous to realise only in case of complex reconstructions of SLG, where old power lines are replaced with new ones. The advantage is that the maximum charging power is always available. It is given by the maximum current carrying capacity of the branch and the used charging stations. The power of the charging stations is independent of the lights. This, of course, applies if the power line of the public lighting switchboard is sized for the maximum charging power of the lamps and charging stations in the branches.

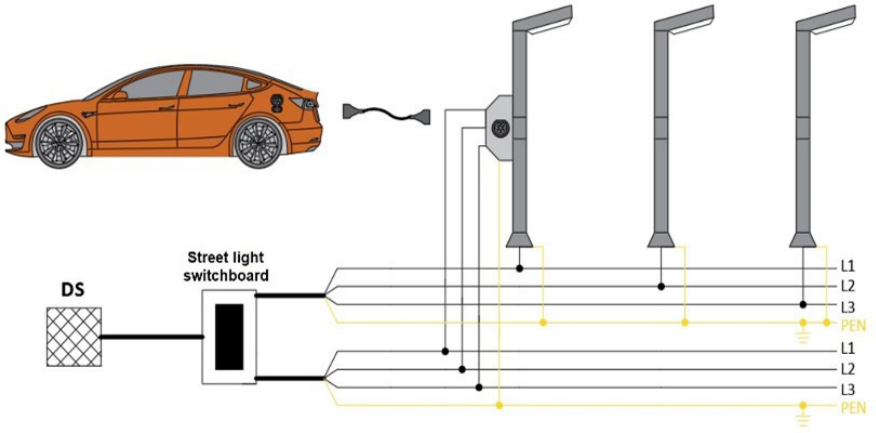

Figure 4: *Charging station powered from a separate power line*

A specific case of the previous option is the connection of an SLG line and a line for charging stations at their ends. This creates a two-side power supply system, which can have a positive effect, for example, to reduce voltage drops, but this system requires luminaires with remote switching on the system.

2.4 Voltage drop

The design of an SLG requires taking care of voltage drop, because it has long distance of power line. The same holds for the implementation of charging stations, but the power load is higher. There is no general Standard that defines the maximum value of the voltage drop in the SLG. The EN 50160 [4] Standard defines a specific voltage deviation of ± 10%, which, at a nominal voltage of 230 V, is in the range of 207 V to 253 V. However, this Standard is only for distribution grids, and defines the SLG voltage only at the power supply point. In Slovakia, the STN 332130 [3] Standard defines the maximum voltage drops for building a lighting installation. Due to the similar indoor appliances and public lighting, it is used in practice as an approximate problem in the calculation of voltage drops in the public lighting network. According to this Standard, the voltage drop in the SLG does not exceed 4% of the nominal voltage from the switchboard to the appliances.

2.5 Calculation of voltage drop

There are several ways to calculate voltage drops. In the calculations, a simplification is used so that the entire load is at the end of the line. This simplification represents the worst possible

situation. For the following calculations, relation (2.1) is from STN 332130, which is for three-phase circuits. This is adjusted to relation (2.2), because the goal of the calculation is to determine the maximum lengths of the power lines by using standard cable cross-sections and a maximum voltage drop of 4% of the nominal voltage value.

$$\Delta U = \frac{\sqrt{3}\,.l.I.PF}{\gamma\,.\,S} \tag{2.1}$$

$$l = \frac{\Delta U\,.\gamma\,.S}{\sqrt{3}\,.I.PF} \tag{2.2}$$

Where:

γ – wire conductivity

ΔU – voltage drop

S – cross-section of wire

l – length of line

I – current in power line

PF – power factor

The result of the calculation is a graph showing the standard copper (CYKY) and aluminium (AYKY) cable lines used in public lighting networks. It is considered with their maximum current capacity and location in the ground.

In the next graph, the CYKY-J 4x10 means a cable with copper core with 4 wires, where 3 wires are for phases, and one is for PEN (neutral N together with protective earth PE). The cross-section is 10 square millimetres.

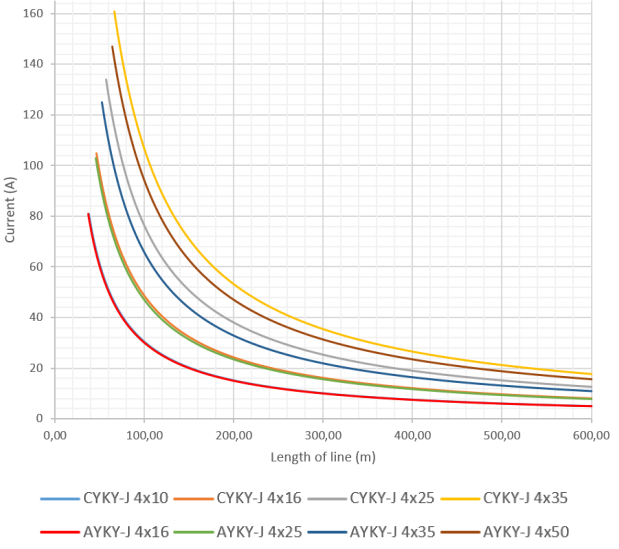

Figure 5: *Dependence between maximum current and length of line for 4% voltage drop and variable cables. Copper (CYKY) and aluminium (AYKY)*

In the graph, the CYKY-J 4x10 means a cable with a copper core with 4 ,where 3 wires are for phases, and one is for PEN (neutral N together with protective earth PE). The cross-section is 10 square millimetres

3 RESULTS

The case study deals with several variants of connecting charging stations to the public lighting network. It determines how far from the SLG switchboard the charging stations can be connected, or how many can be placed in a branch with different cable lines, and the voltage drop is no higher than 4% of the nominal voltage. In this case study, all variants were based on the complex formula (3.1) to calculate the voltage drop. It takes into account the distribution of the current load Ii in the chosen distances of the branch li, based on the sum of the current moments.

$$\Delta U = \frac{\sqrt{3} \cdot \sum_{i=1}^{m} I_i \cdot l_i \cdot PF}{\gamma \cdot S} \tag{3.1}$$

In Tab. 1 and Tab. 2 are the maximum lengths of cable lines from the switchboard, where the charging station can be placed, and the voltage drop has not exceeded the Standard requirements (4%). For the first variants the powering is from one phase according to Fig. 6.

Table 1: *Maximal length of line – variant 1*

One charger **3.7kW** (1x16A, 230V) connected to one phase without luminaire**s**								
Wire	CU 4x10	CU 4x16	CU 4x25	CU 4x35	AL 4x16	AL 4x25	AL 4x35	AL 4x50
Max. length of line (m)	190	304	474	664	188	293	411	587

Table 2: *Maximal length of line – variant 1*

One charger 7.4kW (1x32A, 230V) connected to one phase without luminaires								
Wire	CU 4x10	CU 4x16	CU 4x25	CU 4x35	AL 4x16	AL 4x25	AL 4x35	AL 4x50
Max. length of line (m)	95	152	237	332	94	147	205	293

In this case the charger uses different phase like luminaires. The current in the phase is independent on the luminaires`operation. The length for a 7.4kW charger is shorter, equivalent to the power.

The third variant is powered according to Fig. 7. In this case there are luminaires with an input power of 50 W every 25 metres for a typical situation [7]. The charger and luminaires are connected to all three phases. In this case, we try to simulate the operation with luminaires. The length is calculated only for one charger with full power.

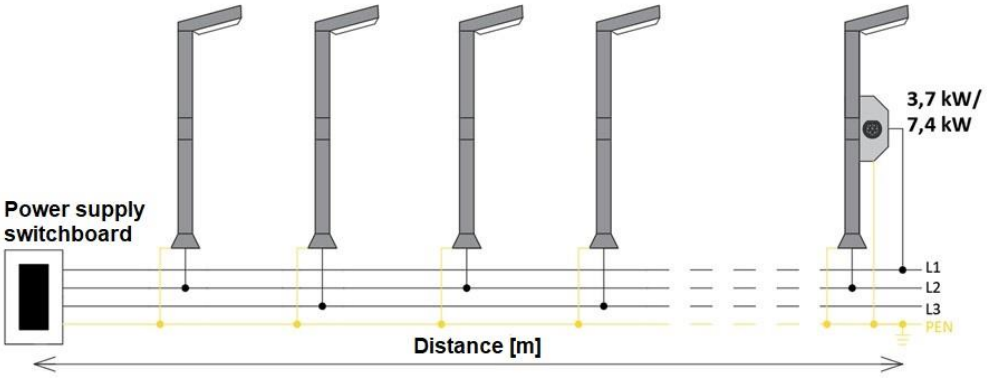

Figure 6: *Connection of charger for variant 1 and 2 (charger a different phase like luminaires)*

Table 3: *Maximal length of line – variant 3*

One charger **22kW** (3x32 A) connected to three phases with luminaires every 25m								
Wire	CU 4x10	CU 4x16	CU 4x25	CU 4x35	AL 4x16	AL 4x25	AL 4x35	AL 4x50
Max. length of line (m)	94	149	233	326	93	144	202	287

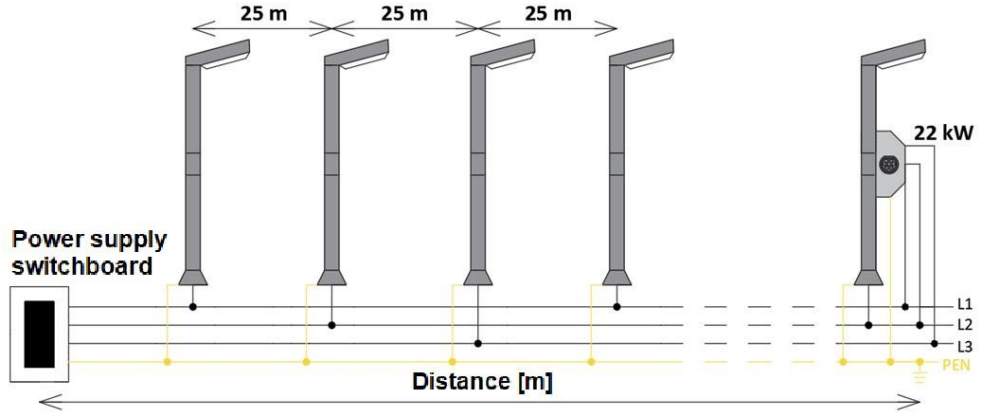

Figure 7: *Connection of charger for variant 3 and 4 (luminaires are on)*

The fourth variant has the same wiring as the third, but the charging station is located at half the distance compared to the third variant.

Table 4: *Maximal length of line – variant 4*

One charger **22kW** (3x32 A) connected to three phases with luminaires every 25m**, with the charger connected in the middle of the line**								
Wire	CU 4x10	CU 4x16	CU 4x25	CU 4x35	AL 4x16	AL 4x25	AL 4x35	AL 4x50
Distance to charger (m)	47	74,5	116,5	163	46,5	72	101	143,5
Max. length of line (m)	925	1225	1525	1825	925	1225	1450	1750

4 DISCUSION

Comparing the second and third variants, we see that the distance difference when using the power line is minimal. So, in the model example, it does not make a significant difference whether the charging station is powered from a dedicated phase that does not power the lights, or is powered from a phase that powers the lights in addition to the charging station. The reason is that the power consumption of luminaires is significantly less than the consumption of the charger. A more significant difference can occur if the consumption of the lights is comparable to the power input of the charger (e.g. old luminaires with high consumption).

The aim of the fourth variant is to show that the maximum length of the power lines is increasing significantly when the charging station is moved from the end of the branch (variant 3) to half the distance (variant 4). Because the charging station is an appliance with a significantly higher power consumption compared to modern LED luminaires, the total lengths of the branches in variant 4 are, in some cases, up to 10 times larger than in the case of variant 3.

Dependence between the number of chargers and the distance from the switchboard

In terms of load, a 7.4kW charging station connected to one phase is equivalent to a 22kW charger connected to three phases. In both cases, the power per phase is the same. Tab. 5 shows how many chargers can be installed at distances of 50, 100, 200 and 300 metres from the switchboard. The consumption of luminaires is not taken into account. In residential areas, the consumption of LED lamps is significantly less than the consumption of the charging station [5].

The closer the charging stations are to the switchboardthe more there can be. Cross-sections CU10 and AL16 are not suitable for maximum load (7.4kW one phase or 22kW three phase) and have limited options for powering the light. If it were necessary to install charging stations at distances greater than 200 metres, it would be worth considering the use of even larger cable conductor cross-sections than those shown in Tab 5.

Table 5: *Number of chargers without luminaires*

Maximum number of chargers (7.4kW one phase or 22kW three phase) without luminaires								
Wire	CU 4x10	CU 4x16	CU 4x25	CU 4x35	AL 4x16	AL 4x25	AL 4x35	AL 4x50
50m from switchboard	1	3	4	5	1	2	3	4
100m from switchboard	0	1	2	3	0	1	2	2
200m from switchboard	0	0	1	1	0	0	1	1
300m from switchboard	0	0	0	1	0	0	0	0

There is a possibility to increase the number of charging stations in the branch and increase the sum of installed power of the charging stations, but this requires intelligent control, that redistributes the available current capacity for the charging stations [6]. During simultaneous charging of electric vehicles from several charging stations in the branch, it is necessary to limit their output power, so that the current capacity of the branch is not exceeded.
The last example is the consideration of a 500m long branch. This branch contains luminaires every 25m. The connection is implemented as in Fig. 7. The first charging station is located at a distance of 25m and each subsequent 25m further.

Table 6: *Number of chargers for a 500m line*

Number of 22kW chargers in a 500m line with 100W luminaires every 25m. The chargers are connected in distance of 25, 50, 100, 150m								
Wire	CU 4x10	CU 4x16	CU 4x25	CU 4x35	AL 4x16	AL 4x25	AL 4x35	AL 4x50
Number of chargers	2	2	3	4	2	2	3	4

Tab 6 shows how many chargers can be connected to a 500m line. When the chargers are every 25m, which means every pole, there can be only 2 to 4 chargers, but relatively close to the switchboard (25m to 100m). The result is that the charger is not easy to connect at a long distance from the switchboard on an existing SLG.

5 CONCLUSION

Currently, there are several professional and scientific articles focused on charging stations. However, the charging stations associated with the SLG operation are addressed minimally. The goal was to provide comprehensive information about charging station operation and implementation methods. It can be connected to existing networks, as well as newly built ones. The electrical connection can be single-phase or multi-phase. The choice of a suitable solution depends on the chargers used, and also the method of operation of the SLG. This paper provides a description of the theoretical level, and a case study focused on the issue of the distance

between the charging stations and the switchboard (or power supply point). Because charging stations have a significant consumption compared to luminaires, inappropriate placement and connection of the charging station can shorten the power line. The calculations consider the nominal power of the charging stations. By using charge management (reducing the input power of the charger), the number of installed chargers increases, but, on the other hand, the charging time increases.

As part of research on this topic the authors have carried out several measurements. The results were processed step by step, and will be published in the following publications. The aim of these measurements will be for providing a base to the theoretical level and showing the risks and potential of SLG in connection with charging stations.

ACKNOWLEDGMENT

This paper is supported by the agency VEGA MŠVVaŠ SR under Grant No.: VEGA1/0390/23.

References

[1] EN 61851-1 *Electric vehicle conductive charging system. Part 1: General requirements*

[2] EN 62196-1 *Plugs, socket-outlets, vehicle connectors and vehicle inlets - Conductive charging of electric vehicles - Part 1: General requirements*

[3] STN 33 2130 *Electric engineering regulations. Internal electric distribution lines*

[4] EN 50160 *Voltage characteristics of electricity supplied by public electricity networks*

[5] **T. Novak, J. Sumpich, J. Vanus,K. Sokansky, R. Gono, J. Latal, P. Valicek**: *A model for predicting energy savings attainable by using lighting systems dimmable to a constant illuminance*, (2020) Lecture Notes in Electrical Engineering, 554, pp. 860 – 869 DOI: 10.1007/978-3-030-14907-9_83

[6] **L. Kuncicky, T. Novak, K. Sokansky, Z. Slanina:** *Road Lighting Control Options*, (2019) Proceedings of 44th WILGA Symposium on Photonics Applications and Web Engineering, Wilga, POLAND, MAY 26-JUN 02, 2019, DOI: 10.1117/12.2536886

[7] **J. Škoda and M. Motyčka**: *Lighting Design Using Ray Tracing*, 2018 VII. Lighting Conference of the Visegrad Countries (Lumen V4), 2018, pp. 1-5, doi: 10.1109/LUMENV.2018.8521111.

[8] **C. Suarez and W. Martinez:** *Fast and Ultra-Fast Charging for Battery Electric Vehicles – A Review*, 2019 IEEE Energy Conversion Congress and Exposition (ECCE), 2019, pp. 569-575, doi: 10.1109/ECCE.2019.8912594.

[9] **T. Chen et al.**: *A Review on Electric Vehicle Charging Infrastructure Development in the UK*, in Journal of Modern Power Systems and Clean Energy, vol. 8, no. 2, pp. 193-205, March 2020, doi: 10.35833/MPCE.2018.000374.

Journal of Energy Technology

JET Volume 16 (2023) p.p. 29-40
Issue 4, 2023
Type of article: 1.01
http://www.fe.um.si/si/jet.htm

INFLATIONARY ELEVATED ENERGY PRICES AS THE MAIN FACTOR OF FUELLING ECONOMICALLY VIABLE ELECTRICITY PRODUCTION IN EU FOSSIL FUELS BASED THERMAL POWER PLANTS

INFLACIJSKO POVIŠANE CENE ENERGIJE KOT GLAVNI FAKTOR POSPEŠEVANJA EKONOMSKO UPRAVIČENE PROIZVODNJE ELEKTRIČNE ENERGIJE V EU FOSILNO GORIVNIH TERMOELEKTRARNAH

Martin Bricl[✉]

Keywords: electricity production, elevated energy prices, fossil fuels, economically viable energy production, thermal power plants

Abstract

The inflation in the last two years has driven the prices of the materials, goods as well as energy significantly higher. With steep increased inflation from month to month in the last two years, the overall inflation peaked at 9.2%, and core inflation at 6.2% in 2022 for the Eurozone area. This elevated prices are troubling the markets, industry and households, making the everyday business much more difficult for them than it was in pre-inflationary times. Also, additional geopolitical changes happened in the last two years (the war in Ukraine) which impacted the energy supply

✉ Corresponding author: dr. Martin Bricl, mag.inž.str., E-mail address: martin.bricl@student. um.si

from the east significantly , primarily lowering the inflow of Russian gas to the European states to almost zero and banning the Russian crude from the international markets. This demanding condition on the energy market, as well as the very narrow time frame for building up a sufficient supply of energy for the winter of 2022 resulted in rather unexpectedly favourable conditions for energy generation (electricity or heat) from still operating coal based thermal power plants, which, in some way, is unacceptable, since we are exiting the coal based thermal power plants in EU actively, and trying to substitute them with renewables & alternatives. However, the aforementioned international markets stress test revealed that abandoning the fossil fuels from our everyday life will not be that easy, as we thought a decade ago.

Povzetek

Inflacija je v zadnjih dveh letih bistveno dvignila cene surovin, blaga in energije. Z močno naraščajočo inflacijo iz meseca v mesec v zadnjih dveh letih je skupna inflacija leta 2022 za območje evra dosegla najvišjo vrednost pri 9,2 %, osnovna inflacija pa pri 6,2 %. Te povišane cene povzročajo težave trgom, industriji in gospodinjstvom, ki jim otežujejo vsakdanje poslovanje. V zadnjih dveh letih so se zgodile tudi dodatne geopolitične spremembe (vojna v Ukrajini), ki so močno vplivale na oskrbo z energijo z vzhoda, predvsem so zmanjšale dotok ruskega plina v evropske države na skoraj nič in privedle do prepovedi izvoza ruske surove nafte na mednarodne trge. Te zahtevne razmere na energetskem trgu in zelo ozek časovni okvir za vzpostavitev zadostne zaloge energije za zimo 2022, so povzročile precej nepričakovano ugodne razmere za proizvodnjo energije (elektrike ali toplotne) iz še delujočih termoelektrarn na premog, kar je nesprejemljivo, saj EU aktivno opušča proizvodno električne energije iz termoelektrarne na premog in jih poskušamo nadomestiti z obnovljivimi viri in alternativami. Vendar pa je že omenjeni stresni test mednarodnih trgov pokazal, da opustitev fosilnih goriv iz našega vsakdana ne bo tako preprosta, kot smo mislili pred desetletjem.

1 INTRODUCTION

The changed conditions on the international markets are the main driver for the completely new outlook with regard to the energy production in the Eurozone area. With closed pipelines for gas from Russia towards Europe and limited Russian crude purchases due to international sanctions, the European Union was, in early 2022, in a tough position regarding the supply of electricity & heat for the domestic markets. With searching for an alternative supplier of the gas from Africa, the Americas and the Middle East, the EU started, or intensified, already operational production from its coal fired thermal power plants, in order to supply a crucial part of the electricity for the domestic market during the winter of 2022. The unexpected inflation emerged during that same time, being only transitional phenomena according to the reassurances of the FED and ECB. Nevertheless, that was not the case, as core inflation peaked at 9.2% and 6.2% correspondingly. This was a surprise for us all, and also for the market regulators who admitted their mistake at the time. The combination of both occurrences resulted in completely new market conditions with elevated prices overall, that made it possible for the thermal power plant to operate within green numbers for them, despite higher fuel, operation, maintenance and carbon dioxide allowances costs. Moreover, even the oil based thermal power plants operated in green numbers, which was a surprise for the energy market, since we are all working actively on the green transition, shifting our energy production from fossil fuels towards renewables and alternatives.

2 CHANGED MARKET CONDITIONS

2.1 Spike in coal spot prices

As described in the introduction, the changed market condition contributed to the situation, where there was enough of a price elevation for the fossil fuel based thermal power plants to operate within the profitable area for them. With the price of electricity, also the price of fuel and operation & maintenance costs increased significantly. Below, in Figure 1, the spot price for the Newcastle coal is shown, where the spike in the price is seen [1] during the period of 2020 – 2023, which was driven mainly by the inflation pressures on the spot price, as well as very high demand for the particular coal, since thermal power plants were getting into the process of start-up. Newcastle coal is thermal coal exported out of the port of Newcastle (FOB) in New South Wales, Australia. It is the price benchmark for the seaborne thermal coal in the Asia-Pacific region, and is exported worldwide as primary fuel for the thermal power plants.

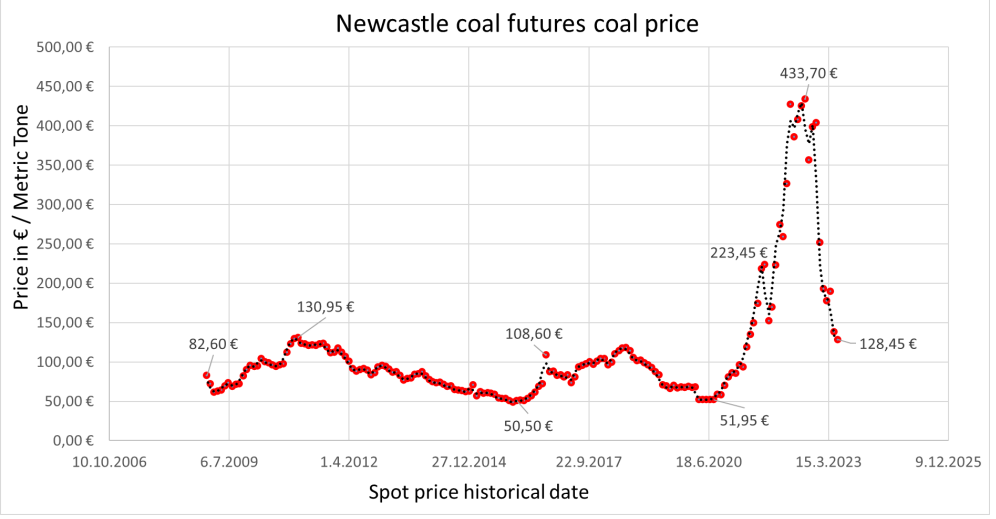

Figure 1: *The movement for the Newcastle Coal spot price. Note the spike in the spot price during 2020 to 2023. The spike was fuelled because of elevated inflation during this time, as well as the elevated demand for the coal, since the thermal power plants were backing the grid electricity consumption due to low production from gas powered power plants.*

From Figure 1 we can observe that the spot price of Newcastle coal increased from its low price of 51,95 € per metric tonne to 433,70 € per metric tonne, meaning that the purchase price of the primary fuel for the operating power plant went up by a factor of 8,3. Consistent with the measures from the central banks to slow and lower the inflation is also the decrease of the Newcastle coal spot price, where normalization of the price took place in the first two quartiles of 2023. Nevertheless, the elevated purchase prices for the coal persisted for almost two years, making the operators of the thermal power plants look very closely for the changes in coal spot prices, to secure the most advantageous price when ordering coal.

2.2 Higher maintenance and operational costs

The operational costs of the conventional thermal power plants have risen significantly, due to the higher costs of the fuel and carbon emission allowances, which two present the main reason for the higher operational cost of the thermal power plants. However, also significant is the increase of the cost of the human labour. Due to inflationary pressures on the wages, the average personal income within the European Union increased by 4.4% in 2022, resulting in additional increases in operational costs. In Figure 2, the Eurostat labour cost levels [2] are presented on the EU map.

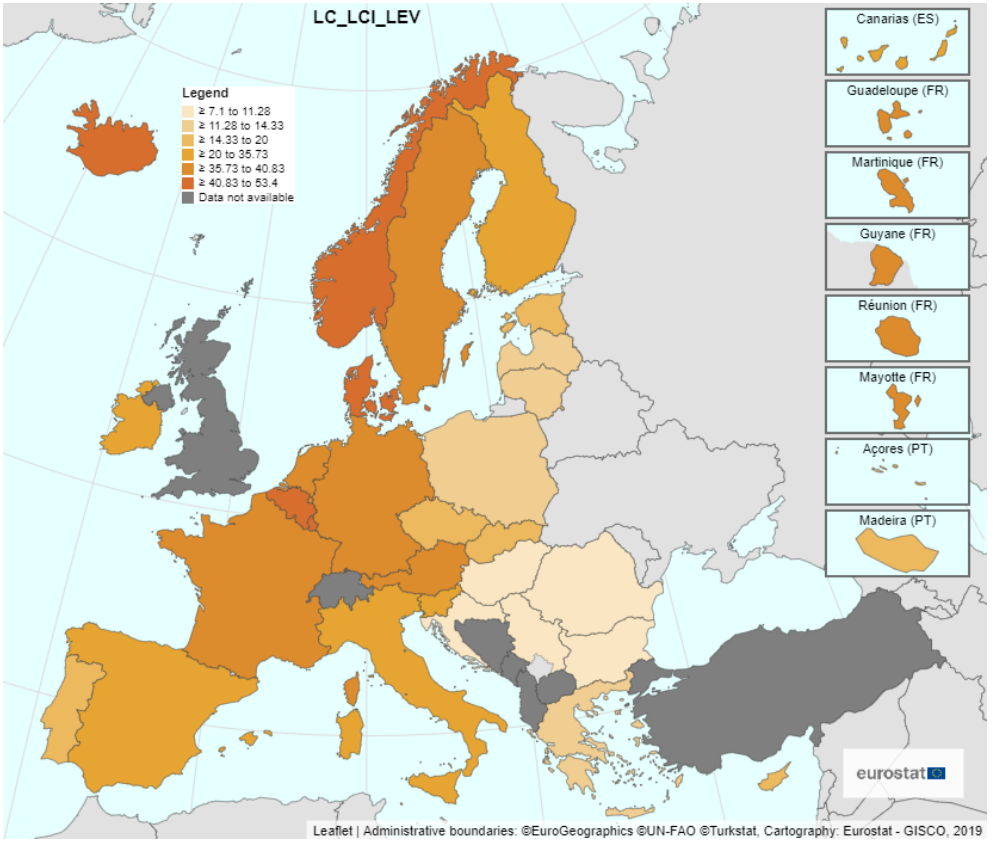

Figure 2: *The cost of labour within the EU. The densest orange colour marked countries have the highest labour cost within the EU. The labour cost ranges from 7,1 €/hour as the lowest average value to 53,4 €/hour as the highest average value (compensation of employees, plus taxes, minus subsidies). The average labour cost is averaged across all sectors of the industry, and is not only focused on the energy production sector. From Figure 2 we can observe that Iceland, the Netherlands, Denmark & Norway have the highest labour costs.*
The source: https://ec.europa.eu/eurostat/databrowser/view/LC_LCI_LEV/default/map?lang=en&category=labour.lc.lcan.

2.3 Price of carbon emission allowances

Carbon emission allowances are also an additional cost to the end price of the electricity producers from the fossil fuels. The price of carbon emission allowances dictates the market, and it is dependent on the asking - offer performance of demand. Within the European Union the European Commission is releasing the carbon emission allowances (coupons) as well, as it is also the regulator for that particular market. In Figure 3, the price movement for the carbon emission allowances [3] is presented for the time period from 2010 to 2023.

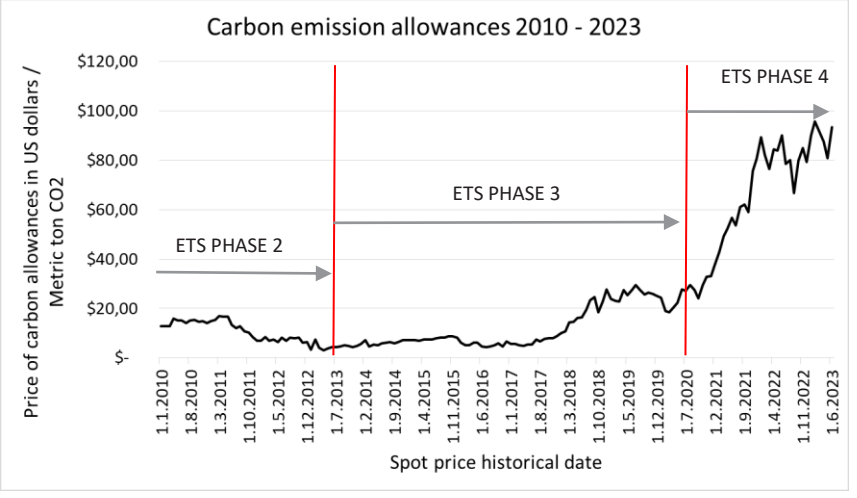

Figure 3: *The movement of the spot price for carbon emission allowances needed for the operation of thermal power plants within the EU ETS.*

From the price movement in the presented graph we see that it is independent of the current international market conditions, since it is regulated as a cap-and-trade market. The rise in the price is achieved by limiting the number of issued and available allowances in every session of releasing the new allowances by the regulator. The spot price of the carbon emission allowances in phase 4 ETS has been fluctuating (after the significant rise of the price) in the area between 70 US dollars – 100 US dollars for a metric ton of emitted carbon dioxide into the atmosphere. The elevated prices of the carbon emission allowances are putting significant pressure on the operational costs of the thermal power plants, making it very difficult for them to operate economically positively. Nevertheless, the high electricity prices on the market were allowing the thermal power plants to operate economically positively within the two-year time period, despite the mechanisms in place to exit the coal-based electricity production gradually in the EU and G-20 countries. The EU regulators are in the process of discussion as to whether the governments across the EU shall also implement the carbon emission taxation for households – the suggested taxation could include additional taxes on the fuel for the transportation & heating of the households. That should give an additional boost to the green transition within the EU, but the regulators were quickly reminded that a lot of people could not afford this kind of additional expenses in the shape of new taxation, since the last overall inflation data for June 2023 is remaining at a high 5,5%, weakening the purchase power of the average European household

from month to month. Because of that, there is not likely to be pressure from the EU regulators for the aforementioned taxation for now.

3 CRUCIAL ROLE OF THERMAL POWER PLANTS

3.1 Changed energy market conditions

After the first price elevation the normalisation of electricity price was performed, mainly because of the cap regulated electricity price, decided by the governments. Gradually, the cap on the electricity prices is expected to be removed. However, the prices of electricity can stay elevated or can even rise further. The reason for that is the EU`s significant increase investment in renewables during the latest energy crisis as a response to the shrinking gas and crude oil imports from Russia. Due to the significant increase of electricity production from renewables, the instability of the grid is rising, making the distribution planning of grid operators even more difficult. That is resulting in a new way for how to adapt to the current energy market conditions, enforcing the electricity end users to change when to save and when to use electricity.

3.2 Thermal power plants crucial for energy supply

In autumn 2022 it became evident that the shrinking supply of the Russian gas and crude would not cover the winter energy needs of Europe. Therefore, the safety plan of putting big thermal power plants [4] back in operation was launched, as presented in figure 4. Consequently, the thermal power plants went from stand-by mode to full operation, resulting in high domestic coal demand. Thermal power plants supplied the electricity as well as needed heat to consumers and end-users, enabling them to save stored gas and oil for later.

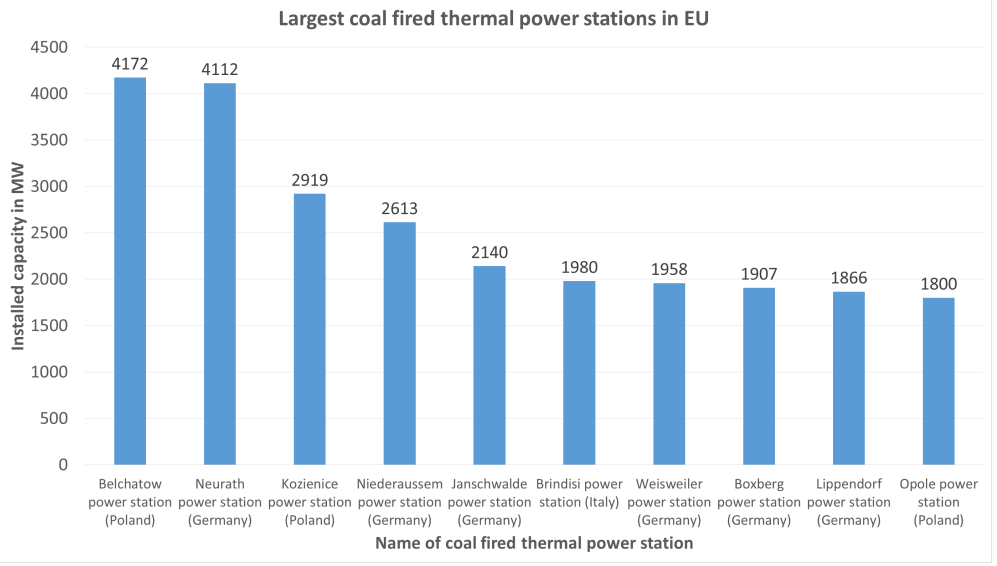

Figure 4: *Largest coal fired thermal power plants in the EU as of 2021.*

Since some nuclear power plants in the EU, particularly in France, were in regular maintenance shut down procedure during that time, the coal fired thermal power plants backed Europe's

electricity network and prevented it from collapse. From that aspect, the coal fired thermal power plants had a crucial role in energy supply, as well as stabilising the distribution network, proving once again that they are very important for our energy supply, and that they should stay in the energy mix for the foreseeable future.

4 COAL AS AN ECONOMICALLY VIABLE FUEL

4.1 Price of electricity as the positive impact factor

The electricity price averaged from the lowest position in February, 128,78 €/MWh to 469,35€/MWh in August 2022, making more than 3 times higher prices during the summer months. The high peak of the electricity sale price has, consequently, boosted the thermal power plant operation into the economically positive area, despite elevated fuel and carbon emission allowances costs. The average monthly electricity wholesale prices in the EU are presented in Figure 5 [5].

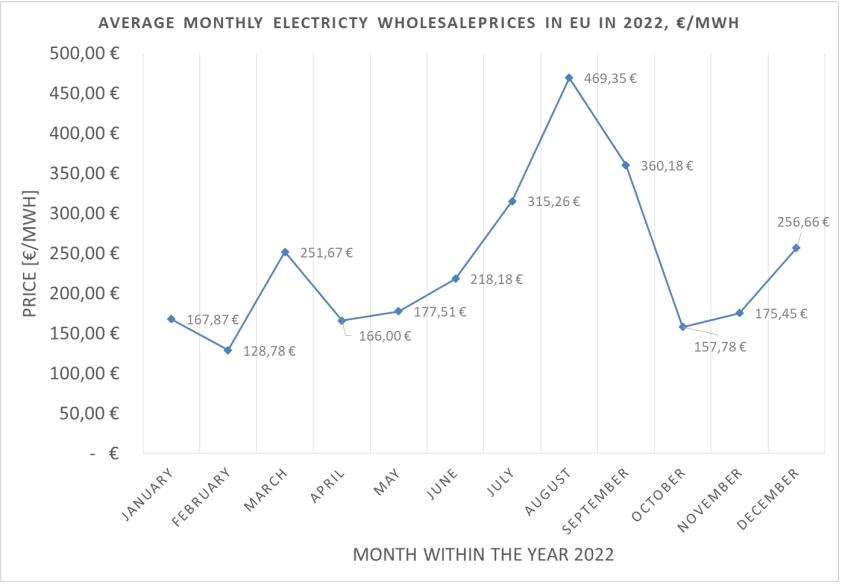

Figure 5: *Average monthly electricity wholesale price in the EU in 2022, €/MWh.*

The high electricity prices have caused the needed action from the governments in order to determine the price cap for households & industry to maintain the normal electricity prices. That action was crucial to keep the industry in good shape and not exposed to the high energy prices too much. The cap also enabled the households to cope through the winter, when the energy usage is higher, especially in the cooler parts of Europe.

4.2 Elevated costs of fuel & carbon emission allowances

The prices of the coal have been elevated during 2022, mainly as the result of the lower imports of gas and crude from Russia. Some EU countries decided that it was best to start the thermal

power plants for the time being, and to wait for the situation to be stabilised on the energy market. The applicable input factors for the thermal power plant operation evaluation are presented in Table 4.1 below.

Table 4.1: *Main applicable input factors for the calculation of the economic performance for an example thermal power plant.*

Input Factor	Quantity	Unit
Peak Coal Price	433,70	€/t
Carbon Emission Allowances	100,00	€/t
Boiler Fuel Consumption	6,30	kg/s
Generated CO2 Emission	0,87	kg/kWh
Operation & Maintenance	43	€ / kWh installed

4.3 Thermal power plant economic performance

As aforementioned, a thermal power plant with an installed capacity of 119 MW_e has consumed through the year 2022 altogether 199,221.00 tons of coal. Taking into consideration the assumed average coal price of 433,70 €/t, the total expenditure for fuelling the thermal power plant with coal throughout the year is accounted for at 86,402,199.70 € as presented in Figure 6.

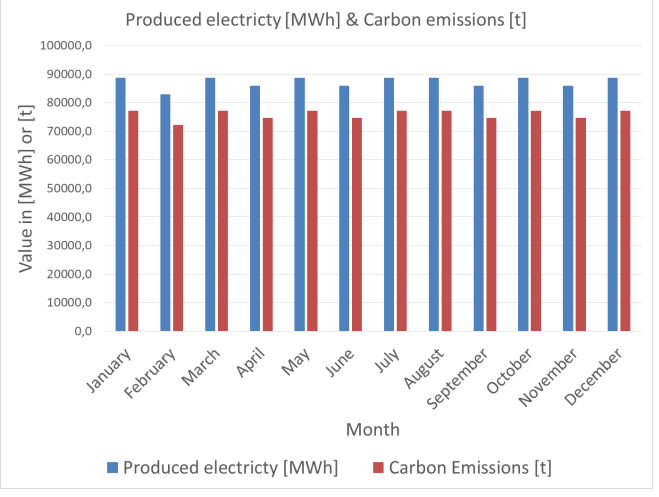

Figure 6: *Produced electricity from a thermal power plant & carbon emissions to the atmosphere.*

Figure 7 is presenting the costs versus monthly expenses for operating the thermal power plant during the 2022 period. The red bars represent the expenses and the green bars the positive net electricity sale by the price that the market dictated. From the Figure it is obvious that the third quarter of 2022 was the most profitable for the thermal power plant operators.

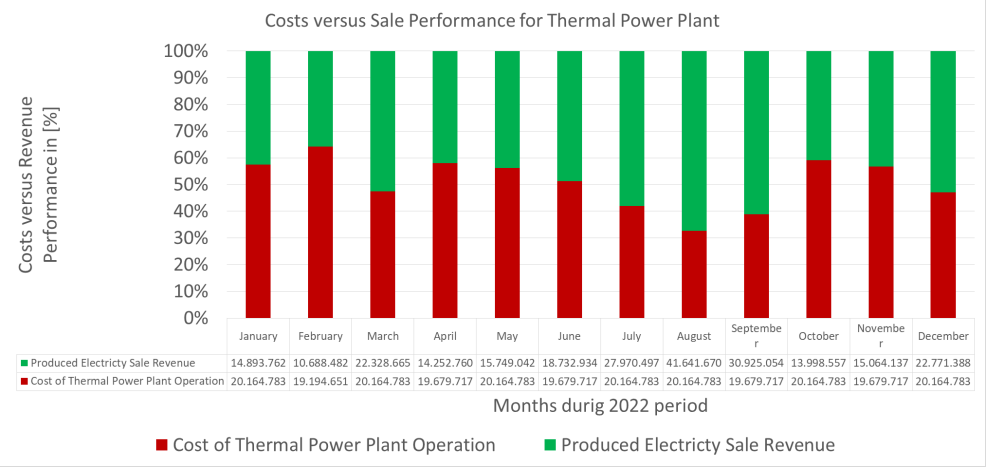

Figure 7: *Costs versus Electricity Sale Performance for a thermal power plant during the 2022 period.*

Figure 8 presents the negative and positive operating months for the thermal power plants and their net monthly result. From the Figure we can see that, for 5 months out of 12 months in the year, the operation of the thermal power plants was positive. Especially positive was the third quarter of the year 2022. The net profit of the observed case was 9.94 million € on a yearly basis.

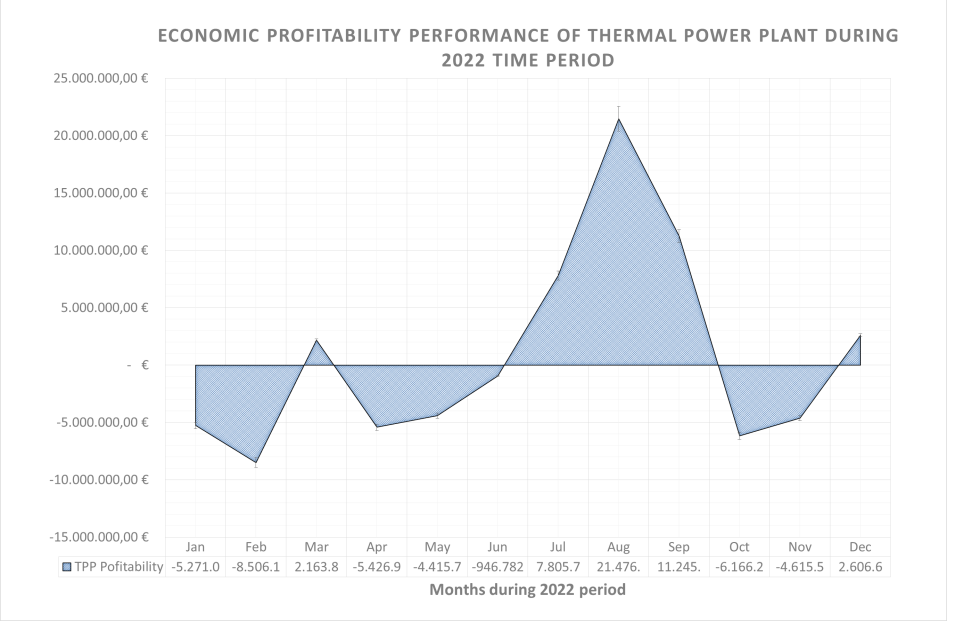

Figure 8: *Economic profitability performance of a thermal power plant during the 2022 time period.*

5 EXITING THE INFLATION & ENTERING THE RECESSION ERA

5.1 Transitory versus lasting phenomena

The starting inflation, being labelled as a transitory one, was present through the major part of 2021. With the beginning of 2022 it was more than obvious that inflationary pressures were starting to accelerate the inflation itself, consequently lifting the core inflation well above 5%. At that point the central banks and other regulators were forced to react to the situation, mainly by lifting the bank rates, but also with some other actions, such as, for example, capping the energy prices, in order to retain the price control across the energy market. Figure 9 below shows the rising of the bank interest rates due to the hard inflation environment [6].

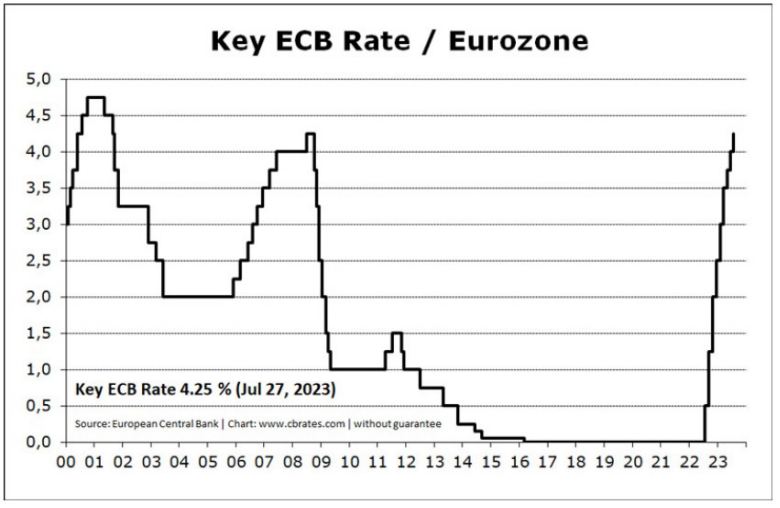

Figure 9: *Rising of the ECB rates during 2022 & 2023 due to inflationary pressures. The source: https://tradingeconomics.com/euro-area/interest-rate.*

5.2 The future aspect of inflation presence

The current elevated interest rates are keeping the prices of material costs as well as other services relatively high. The ask – demand ration has not been restored fully. Therefore, some inflationary pressures are still present, despite raising the interest rates. There are forecasts that, by the end of the year 2023, some additional interest rates raising will be put in place, leading the current market situation towards a stricter monetary policy, with the intention to lower the overall and core inflation to the desired levels by around 2% on a yearly basis. Big efforts by the regulators are in place to avoid a recession at the end of the rates` hikes. Instead of that, a so-called soft landing is expected, meaning that the markets and economy overall will be able to survive the transitionary time of increased interest rates, without shrinking itself and consequently falling into a recession. From the aspect of the raw materials` price movement, the strict monetary policy is expected to slower the ask – demand ratio, leading to the normalisation of the prices. It is crucial to secure the stable prices of the energy sources (derivates) before

the winter 2023 – 2024, since another price spike of the derivates would mean relatively high pressures on the economies of the EU, which are already facing additional problems, such are broken supply chains, elevated cost of the raw materials, and, as aforementioned, elevated costs of the energy. As expected, the recession possibility is increasing further with the less positive market data feedback. Should the current situation continue, an overall recession in the EU economy is imminent, meaning that the conditions for the viable thermal power plant operation will end, mainly because of slower activity of the production industries that will, consequently, consume less energy as a result of the lower goods demand from the market and end customers.

6 CONCLUSIONS

The demanding period of the last few years showed us that, although the green transition is in progress, the dependence on fossil fuels is still very much present in our everyday life. The regulators and decision makers shall establish the system in which the green transition decisions have support – social as well as economical. Returning to the usage of the fossil fuels shall be as crucial backup only in a case of demanding electrical network conditions and when the imminent stabilisation of the network is required. In the last two years the combination of geopolitical and economic factors helped to establish the environment in which the existing thermal power plants with a high CO_2 emission factor were able to operate economically viably, which is in contradiction of the green transition policies. The regulators of the electricity production and distribution shall subsidise the green electricity production, so that it would have economical advantage in comparison with the price of electricity produced in conventional power plants.

References

[1] **Trading economics**: *The movement of Newcastle Spot Price* [online], https://tradingeconomics.com/commodity/coal (2.8.2023)

[2] **Eurostat:** *Labour cost within the EU* [online], https://ec.europa.eu/eurostat/databrowser/view/LC_LCI_LEV/default/map?lang=en&category=labour.lc.lcan (7.8.2023)

[3] **Statista:** *The movement of spot price for carbon emission allowances* [online], https://www.statista.com/statistics/1322214/carbon-prices-european-union-emission-trading-scheme/ (15.8.2023)

[4] **Statista:** *Largest coal fired thermal power plants in EU* [online], https://www.statista.com/statistics/1264199/largest-operational-coal-power-plants-by-capacity-in-the-eu-27/ (18.8.2023)

[5] **Eurostat:** *Average monthly electricity wholesale price in EU in 2022* [online], https://www.statista.com/statistics/1322214/carbon-prices-european-union-emission-trading-scheme/ (20.8.2023)

[6] **Trading economics:** *Rising of ECB rates during 2022 & 2023* [online], https://tradingeconomics.com/euro-area/interest-rate (22.8.2023)

Nomenclature

EU	European Union
FED	Federal Reserve Board
ECB	European Central Bank
FOB	Freight on Board
US	United States
ETS	Emission Trade System
CO2	Carbon dioxide
MWe	Megawatt electric
MWh	Megawatt hour
kWh	Kilowatt hour
t	Tonne
kg	Kilogram
s	Second
%	Percentage
€	Euro

Journal of Energy Technology

JET Volume 16 (2023) p.p. 41-53
Issue 4, 2023
Type of article: 1.01
http://www.fe.um.si/si/jet.htm

ANALYTICAL ESTIMATION OF THE OPTIMAL PV PANEL TILT BASED ON A CLEAR-SKY IRRADIANCE MODEL

ANALITIČNA OCENA OPTIMALNEGA NAGIBA PV PANELA NA PODLAGI MODELA PROUČEVANJA SONČNEGA SEVANJA PRI JASNEM NEBU

Elena Golubovska[1] , Biljana Citkuseva Dimitrovska[2], Roman Golubovski[3]✉

Keywords: PV panel tilt, optimal PV panel inclination, PV conversion efficiency, sun position model, clear-sky solar irradiance model

Abstract

PV panel tilt and sun tracking are crucial aspects of PV conversion efficiency. We propose an analytical methodology for estimation of the optimal PV panel tilt based on calculation of the sun`s position and the application of a clear-sky solar irradiance model. Our methodology outputs three angles referencing a geolocation and the moment of interest: the incidence angle q, the sun altitude a and the sun azimuth z. The irradiance model estimates the solar irradiation at a geolocation that can be used for PV conversion estimation based on specified tilt β. The moment PV power is used for calculation of the daily energy production, and the optimal β is identified in the tilt range of 0° to 90°. Seasonal division of the year is performed, and optimal seasonal tilt is estimated based on the maximally produced seasonal energy, tested with every corresponding β.

✉ Corresponding author: Prof. Dr, Roman Golubovski, UKIM, FNSM, Arhimedova bb, Skopje, N.Macedonia, Tel.: +389 70 206 459, E-mail address: roman@pmf.ukim.mk

1 University Ss. Cyril and Methodius, Faculty of Computer Science and Engineering, Skopje, N.Macedonia

2 University Goce Delcev, Faculty of Electrical Engineering, Shtip, N.Macedonia

3 University Ss. Cyril and Methodius, Faculty of Natural Sciences and Mathematics, Skopje, N.Macedonia

The methodology is tested on four typical seasonal models - 12 months, 4 three-month quarters, 2 half-year seasons and a single optimal annual fixed β The preliminary simulations produced promising results consistent with the practical engineering implementations.

Povzetek

Nagib PV-panela in sledenje soncu sta ključna vidika učinkovitosti PV-pretvorbe. Predlagamo analitično metodologijo za oceno optimalnega nagiba fotonapetostne plošče na podlagi izračuna položaja sonca in uporabe modela sončnega sevanja pri jasnem nebu. Naša metodologija prikaže tri kote, ki se nanašajo na geolokacijo in trenutek opazovanja: vpadni kot θ, višinski kot sonca a in azimut sonca z. Model obsevanja ocenjuje sončno sevanje na geolokaciji, ki se lahko uporabi za oceno pretvorbe PV na podlagi določenega nagiba β. To je trenutek, ko se PV moč uporabi za izračun dnevne proizvodnje energije, optimalni β pa se določi v območju nagiba od 0° do 90°. Izvede se sezonska delitev leta in optimalni sezonski nagib se oceni na podlagi največje proizvedene sezonske energije, testirane z vsakim ustreznim β Metodologija je preizkušena na štirih tipičnih sezonskih modelih – 12 mesecih, štirih trimesečnih kvartalih, dveh polletnih sezonah in enem optimalnem letnem fiksnem β. Predhodne simulacije dajejo obetavne rezultate, skladne s praktičnimi inženirskimi izvedbami.

1 INTRODUCTION

Renewable energies are subject to continuous research for their sustainability, contrary to the depletive and hazardous properties of fossil fuels and nuclear fission. Solar energy is obviously the most sustainable form, independent of other circumstances, until it reaches the atmosphere and is degraded acceptably while propagating through it. Solar irradiation is used efficiently by photovoltaic (PV) conversion, which is the cheapest electrical energy production technology compared to the rest. PV technologies are also affordable at the household level, making them globally popular today. The widespread market sustains a growing PV production industry that increases the PV conversion efficiency continuously and lowers the market costs. However, besides the improved material performances, planners of PV plants also tackle installation efficiency issues for maximizing energy production against lower costs. Among other things, they aim for optimal latitude (L) placement, as well as optimal panel tilt (β) for the sun`s incidence angle (θ) closest to the possible zenith, and longer possible under daylight. The incidence angle θ can be maintained optimally by horizontal azimuth tracking, but the panel azimuth is usually fixed towards local noon (1200h). The panel tilt optimization is subject to vertical inclination adjustment strategies, ranging from fixed tilt throughout the year to daily tracking (involving the use of computers equipped with sensors and actuators, introducing additional costs such as hardware, cabling, maintenance and energy consumption), depending on the economic circumstances. This paper proposes an analytical methodology for estimation of the optimal PV panel tilt based on the estimated sun position defined by the incidence angle θ, the sun`s altitude α and its azimuth z, and application of a clear-sky solar irradiance model. The sun's location is determined [1] against a specified geolocation for a specified date and time. The solar irradiance model [2], unlike efforts estimating locally arrived irradiation based on statistical meteorological data or measurement-based modelling [3] - [15], calculates the maximal possible incoming solar irradiation that can be used for PV conversion estimation considering the latitude placement and sun`s position, as well as the panel tilt β. This allows for momentary power estimation and possible energy production over a specified period. The methodology allows tracking optimal

β on a daily basis (the daily fixed tilt for which maximal daily energy can be produced), or for arbitrary defined seasons (the fixed tilt for which maximal seasonal energy can be produced). This approach is tested on four typical seasonal models - 12 months, 4 three-month quarters, 2 half-year seasons, and a single optimal annual fixed β.

2 SUN POSITION MODEL

The current sun position model calculates the incidence angle θ that the sun`s rays fall under at a specific geolocation (latitude and longitude) in a specific moment of the year (date and time), being the angle between the sun`s ray falling on that location and its perpendicular vertical line, as well as the seasonal sun altitude α and the daily azimuth z. In order to calculate these three essential angles, additional specifics regarding the earth's rotations need to be considered. Figure 1 shows the earth's annual (365.25 days) rotation around the sun, as well as the fixed declination δ of the earth's axis (23.45°), which oscillates with respect to the sun, producing on earth a solar declination angle between ± 23.45° depending on the moment in the year.

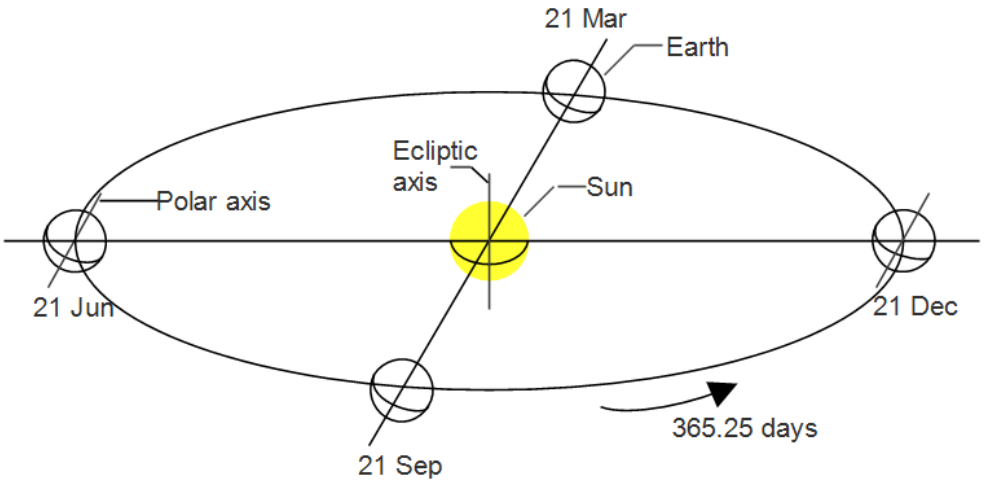

Figure 1: *Annual motion of the earth around the sun*

There are four fiducial dates during the year - 21 Jan (the summer solstice), which is the longest (summer) day in the northern hemisphere; 21 Dec (the winter solstice), which is the shortest (winter) day in the northern hemisphere; and 21 Mar and 21 Sep (the two equinoxes) with equal duration of their day and night. The daily declination δ for day N (of the 365 in a year) according to ASHRAE (the American Society of Heating, Refrigerating and Air-Conditioning Engineers) can be calculated with the expression 2.1.

$$\delta = 23.45° \, sin\left[\frac{360°}{365}(N - 81)\right] \qquad [°] \tag{2.1}$$

The specific moment is defined by the input date and time, expressed as the day N [1~365] in the year, and the local standard time (LST) expressed as local minute time (LMT) [min] in that day. The moment needs to be converted to a current angle with respect to a reference meridian. This means that the specified moment of time needs to be converted from LST to the local apparent solar time (AST), and then to the hour angle h representing that moment. In the local noon, LST should be exactly 1200h (midday), and so should the AST correspond to the solar zenith (1200h). However, during the annual rotation around the sun the earth's path varies, so does its speed around the sun. Due to some specifics, the rotational speed around its own axis also varies. These variations imply two corrections required for acceptable LST to AST conversion. The first one is the "equation of time" (EoT), which considers the eccentricity of the earth's orbit around the sun, and for day N is determined with the expression 2.2.

$$EoT = 9.87\sin(2B) - 7.53\cos(B) - 1.5\sin(B) \qquad [min] \tag{2.2}$$

$$B = (N-1)\frac{360^\circ}{364} \qquad [^\circ]$$

The second correction is the "longitudinal correction" of LST, given in expression 2.3, which represents the current time with respect to a global time zone (T_GMT) or a standard meridian (SM) of the 24 defined for zoning the globe. It takes 4min for the sun to traverse 1°, and LST is "constant" in the watch for the whole 15° (representing an hour from 24 zones). The correction is intended to cancel out the running difference between the local longitude (LL) and the SM. Additionally, the daylight saving (DS) can be considered, expressed in [min] (being 0 when ignored and 60 otherwise).

$$AST = LST + EoT \pm 4(SL - LL) - DS \qquad [^\circ] \tag{2.3}$$

Now, the current hour angle h considering the current AST is given in the expression 2.4:

$$h = (AST - 12)\cdot 15^\circ \qquad [^\circ] \tag{2.4}$$

Having h correspond to the specified date and time, it can be put in the context of the corresponding latitude L, solar declination δ, local zenith Φ, sun`s altitude $\alpha$ and sun`s azimuth z. Figure 2 and Figure 3 depict the context in which the angle parameters correlate. The sun`s altitude α oscillates with the seasonal dynamics, and can be correlated trigonometrically with the local latitude L, the solar declination δ and the hour angle h in expression 2.5.

$$\alpha = sin^{-1}[sin(L)sin(\delta) + cos(L)cos(\delta)cos(h)] \qquad [^\circ] \tag{2.5}$$

The sun`s azimuth z oscillates with the daily dynamics, and can be correlated trigonometrically with the sun`s altitude α, the solar declination δ and the hour angle h in expression 2.6.

$$z = sin^{-1}\left[\frac{cos(\delta)sin(h)}{cos(\alpha)}\right] \qquad [^\circ] \tag{2.6}$$

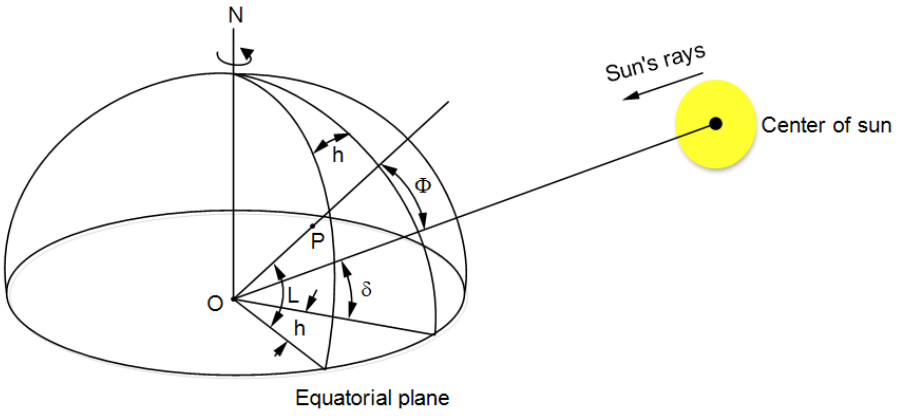

Figure 2: *Definition of latitude, hour angle and solar declination*

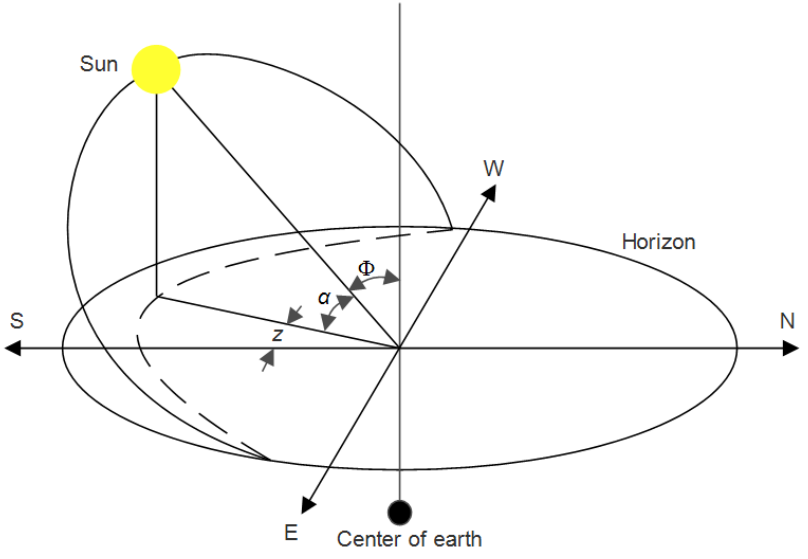

Figure 3: *Solar angles defining its position in the sky along its daily path*

Figure 4 defines the trigonometrical context of the inclined plane. The incident angle θ equals the zenith angle Φ if the plane is not tilted, but for a panel with tilt $\beta > 0°$ and own azimuth fixed toward local noon (0°), expression 2.7 gives the cos(θ) required by the PV conversion model.

(2.7)

$$\begin{aligned} cos(\theta) = {} & sin(L)sin(\delta)cos(\beta) - cos(L)sin(\delta)sin(\beta)cos(Z) + \\ & + cos(L)cos(\delta)cos(h)cos(\beta) + \\ & + sin(L)cos(\delta)cos(h)sin(\beta)cos(Z) + cos(\delta)sin(h)sin(\beta)sin(Z) \end{aligned}$$

3 ENERGY CONVERSION MODEL

The implemented PV energy conversion model is of the "clear-sky" type [2]. The clear-sky solar irradiation model assumes ideal meteorological conditions, where the irradiation of the location of interest is unobstructed by clouds or other atmospheric circumstances. Although not real, such an ideal context is optimal for comparative analysis. The extraterrestrial solar radiation arrives at the outer border of the earth's atmosphere in almost constant intensity, defined as the solar constant G_{SC}. The solar constant is the quantity of solar radiation arriving perpendicular to the atmosphere at an average distance from the sun, with very small variations between different analytical estimations and satellite measurements.

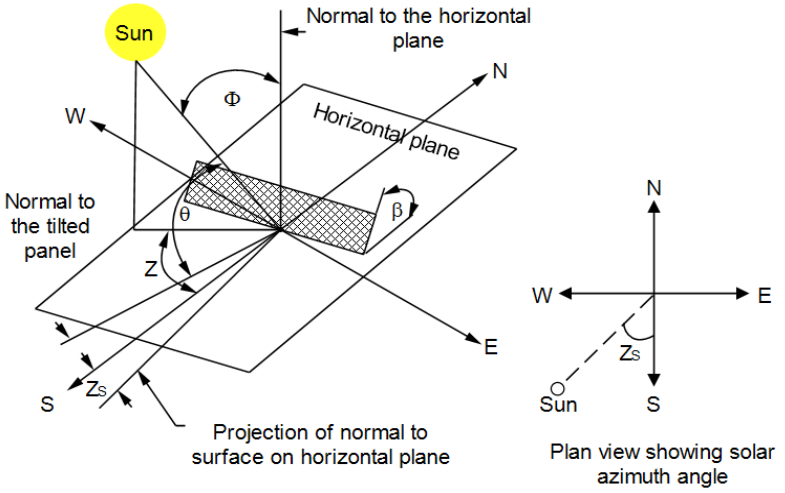

Figure 4: *Solar incidence angle for a non-horizontal surface*

The value used in this paper is 1367 [W/m^2], as proposed by Iqbal (1983) [16]. However, the sun's radiation declines intrinsically with an annual rate of 0.02% (insignificant, and can be disregarded), and varies $\pm$ 3.3% due to the earth's variable distance from the sun, which is significant and must be taken into consideration. This results in the effective arrived radiation at the atmosphere G_{ATM}, expressed for day N of the year according to Spencer (1971) [17] with the following formula:

$$G_{ATM} = G_{SC}\left[1 + 0.033\,cos\left(\frac{360^\circ}{365}N\right)\right] \qquad [W/m^2] \tag{3.1}$$

The direct radiation (beam radiation) G_{DIR} is the amount of irradiation propagated to the location of interest through the atmosphere without dissipation. Diffuse radiation (sky radiation) G_{DIF} is the dissipated irradiation arriving at the location of interest from the surrounding space. The total irradiation G is the amount measured at the location of interest. The energy model is expected to provide an analytical estimation of the PV conversion power, considering the direct and diffuse irradiation and ignoring the reflection component. The PV conversion efficiency η is assumed to be up to 20%, as the commercial PV technologies currently offer. The expression for the PV converted power at the location of interest is:

$$P = \eta\,[(G_{DIR} + G_{DIF})\,S_{DIR} + G_{DIF}\,S_{DIF}] \qquad [W] \tag{3.2}$$

G_{DIR} and G_{DIF} result from the interaction of G_{ATM} with the atmosphere (its vapor molecules and microparticles) while propagating and dissipating through it. This interaction is defined as atmospheric transmittance τ. The transmittance of direct irradiation τ_{DIR} is proposed by Hottel (1976) [18] in the following expression:

$$\tau_{DIR} = a_0\,r_0 + a_1\,r_1\,e^{-\frac{k\cdot r_k}{cos(\Phi)}} \tag{3.3}$$

where Φ is the zenith angle (90° - α), and a_0, a_1 and k are the atmospheric parameters of a clear sky with visibility up to 23 km, and for altitudes (A) of up to 2.5 km, given in expression 3.4:

$$a_0 = 0.4237 - 0.00821\,(6 - A)^2 \tag{3.4}$$
$$a_1 = 0.5055 - 0.00595\,(6.5 - A)^2$$
$$k = 0.2711 - 0.01858\,(2 - A)^2$$

and where r_0, r_1 and r_k are the corrective climate factors declared in Table 1:

Table 1: *Corrective climate factors*

Climate type	r_0	r_1	r_k
Tropical latitudes (0° ≤ L < 23.45°)	0.95	0.98	1.02
Mid latitudes (23.45° ≤ L < 66.55°) in summer	0.97	0.99	1.02
Mid latitudes (23.45° ≤ L < 66.55°) in winter	1.03	1.01	1.00
Polar latitudes (66.55° ≤ L ≤ 90°) in summer (during daylight)	0.99	0.99	1.01

According to the same model, the transmittance of diffuse radiation τ_{DIF} is given in expression 3.5:

$$\tau_{DIF} = 0.271 - 0.294\,\tau_{DIR} \tag{3.5}$$

Knowing both transmittances, τ_{DIR} and τ_{DIF}, allows calculation of the direct and diffuse irradiation that fall perpendicular at the locations of interest, $G_{DIR(n)}$ and $G_{DIF(n)}$, as given in expression 3.6:

$$G_{DIR(n)} = \tau_{DIR}\,G_{ATM} \qquad [W/m^2] \tag{3.6}$$
$$G_{DIF(n)} = \tau_{DIF}\,G_{ATM} \qquad [W/m^2]$$

Knowing the tilt β, and having calculated cos(θ) it is now possible to correct both irradiation components in their final form:

$$G_{DIR} = G_{DIR(n)}\,cos(\theta) = G_{ATM}\,\tau_{DIR}\,cos(\theta) \qquad [W/m^2] \tag{3.7}$$

$$G_{DIF} = G_{DIF(n)}\,\frac{1+cos(\beta)}{2} = G_{ATM}\,\tau_{DIF}\,\frac{1+cos(\beta)}{2} \qquad [W/m^2] \tag{3.8}$$

In expression 3.5 it is obvious that the diffuse component is neglective compared to the direct, so the final expression for the PV conversion power is:

$$P = \eta\,(G_{DIR}\,S_{DIR} + G_{DIF}\,S_{DIF}) \qquad [W] \tag{3.9}$$

Tracing expression 3.9 backwards, it is clear that PV conversion power P at a specified geolocation can be estimated with the clear-sky model and the sun position model for a specified moment in the year by just knowing the date and time.

4 OPTIMAL TILT CALCULATION

Optimal panel inclination is the tilt β for which the panel produces maximal daily energy DE_{MAX}, calculated by integrating its power P in 15min intervals during the daylight of a specified date (N). The algorithm for optimal tilt determination checks (calculates) DE against "all" β values in the range of 0° to 90° with a step of 1°. The tilt that produces DE_{MAX} is the optimal daily tilt β_{OD}. Figure 5 provides the optimal β curves for "all" latitudes in the north hemisphere from 0° (the equator) to 90° (the North Pole) with the step 5°. Every graph corresponds to a latitude labeled with a red horizontal line. Added is the latitude of Skopje (42°).

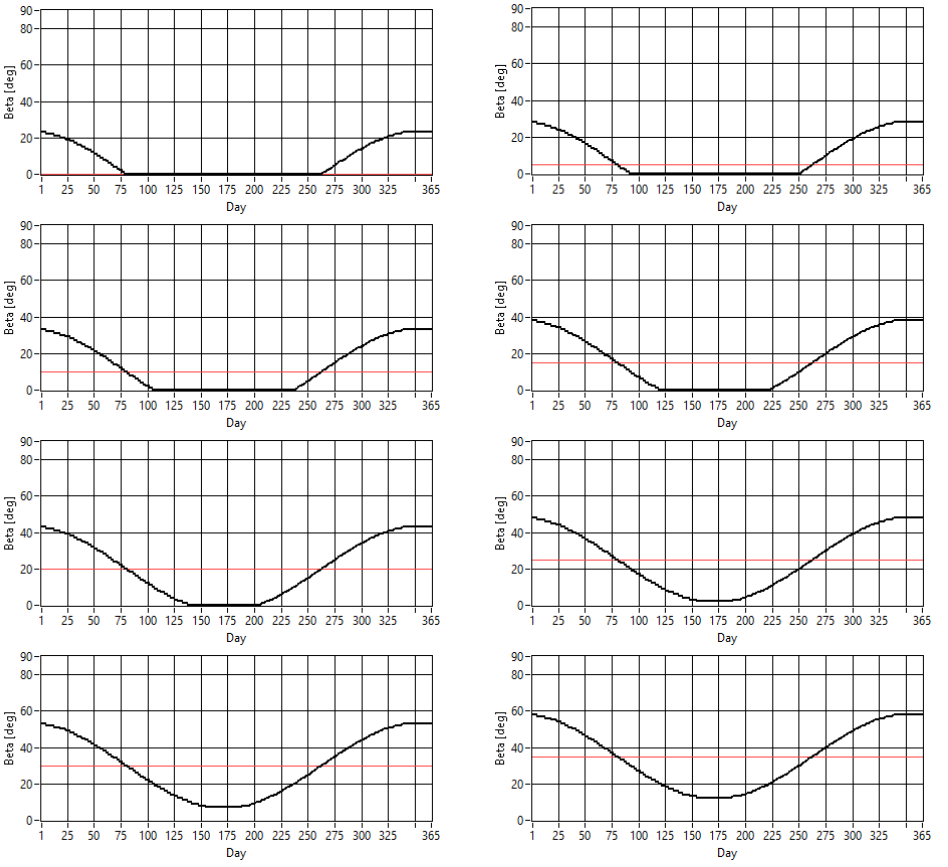

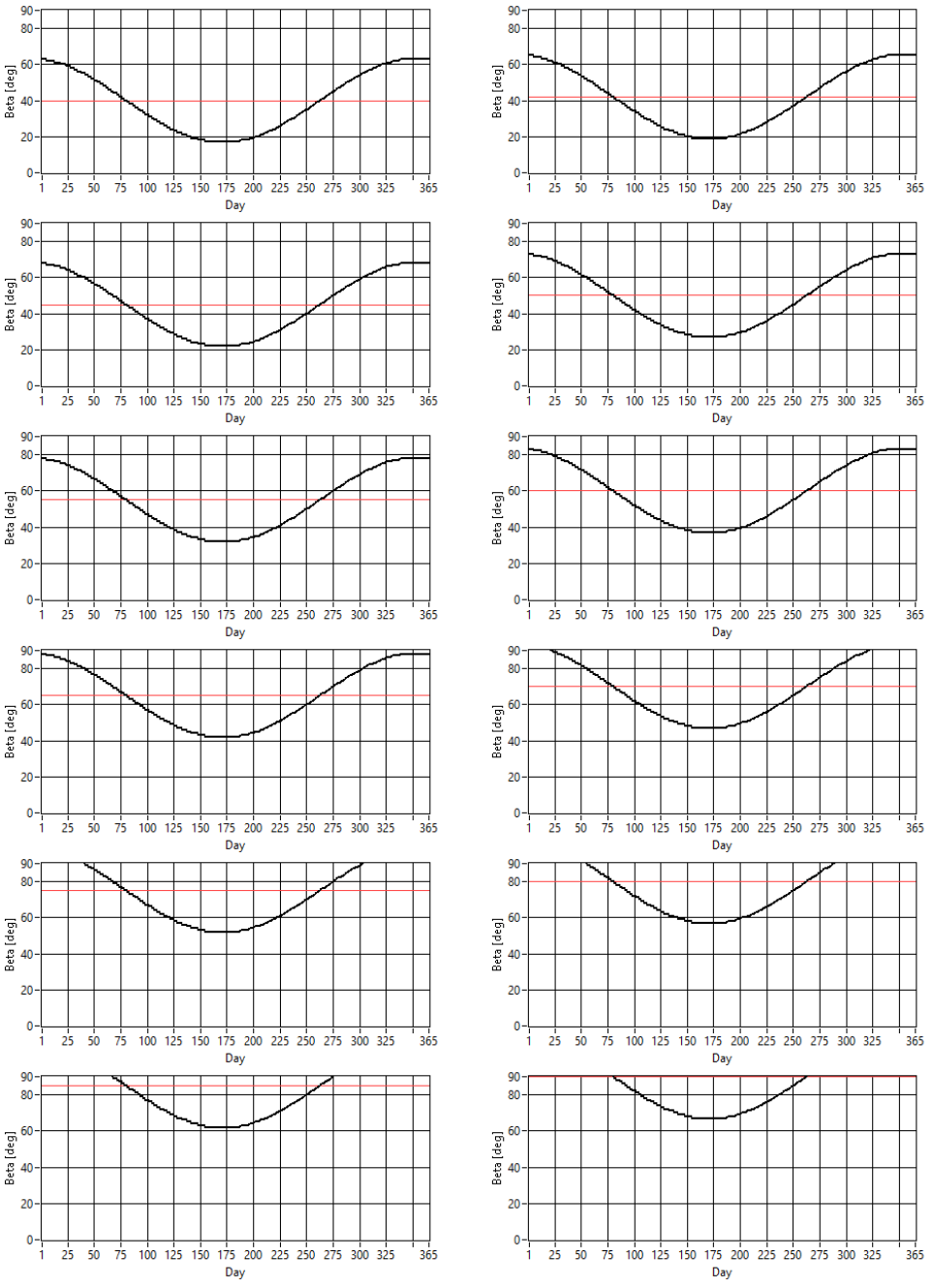

Figure 5: *Annual tracking of the daily optimal tilt for all north hemisphere latitudes from 0 ° to 90 ° with the step 5 ° (including 42 °)*

It is obvious that the tropical curves (0° to 23.45°) are "cut below" at 0°, since, during summer in the northern hemisphere, these latitudes are closer to the zenith than the equator, and the panels are laid on the ground optimally and cannot tilt down anymore. In the mid-latitudes (from 23.45° to 66.55°) the optimal β oscillation of $\pm$ 23.45° is obvious, due to the corresponding oscillation of the solar declination δ. The polar latitudes (above 66.55°) are in daylight half the year also due to δ. Daily tracking (especially for large PV plants) requires the use of computerized equipment (for automatic tilting), that may not always be economically feasible, so the most widespread strategy is seasonal optimization. Being able to calculate optimal tilt β_{OD} for daily tracking allows the determination of seasonal optimal tilt β_{OS}. After an arbitrary season is defined with starting and ending dates, the cumulative seasonal energy SE is calculated for the whole season for every β_{OD} of the embraced dates. When SE_{MAX} is identified, its corresponding β_{OD} is the optimal seasonal tilt β_{OS}. The methodology was tested with four scenarios:

1. Monthly tilting - 12 seasons with optimal tilt
2. Four seasons - defined to have the least possible β_{OD} variation among the embraced days
   S#1 $\rightarrow$ 5 Nov ~ 4 Feb (winter, 92 days)
   S#2 $\rightarrow$ 5 Feb ~ 6 May (spring, 91 days)
   S#3 $\rightarrow$ 7 May ~ 5 Aug (summer, 92 days)
   S#4 $\rightarrow$ 6 Aug ~ 4 Nov (autumn, 90 days)
3. Two seasons - defined to have the least possible β_{OD} variation among the embraced days
   H#1 $\rightarrow$ 21 Sep ~ 20 Mar (winter, 181 days, 21 Dec - centered)
   H#2 $\rightarrow$ 21 Mar ~ 20 Sep (summer, 184 days, 21 Jun - centered)
4. Fixed annual tilt

Table 2 shows the results of the simulation of the four scenarios. The monthly tilting (scenario #1) for all latitudes is presented graphically in Figure 6.

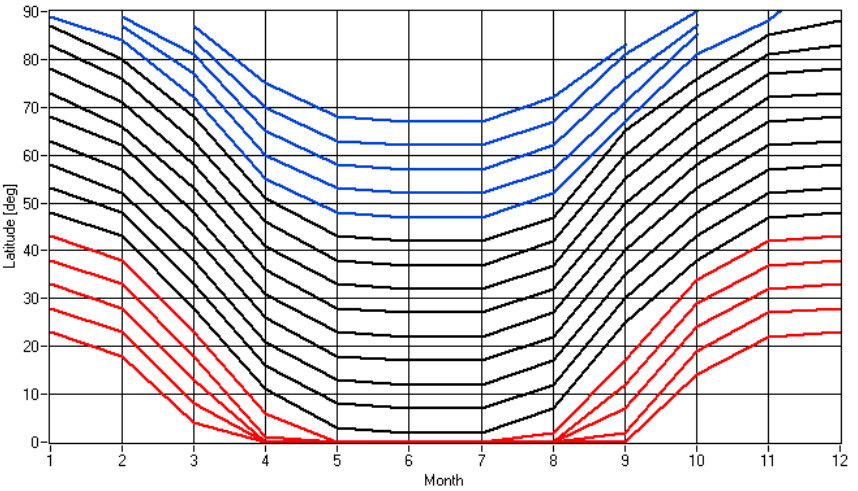

Figure 6: *Annual latitude curves of the monthly optimized tilt*

Table 2: *Seasonal tilt optimization*

Lat	Jan	Feb	Mar	Apr	May	Jun	Jul	Aug	Sep	Oct	Nov	Dec	S#1	S#2	S#3	S#4	H#1	H#2	365
0°	23	18	4	0	0	0	0	0	0	14	22	23	23	0	0	0	21	0	1
5°	28	23	8	0	0	0	0	0	2	19	27	28	28	5	0	5	26	0	5
10°	33	28	13	0	0	0	0	0	7	24	32	33	33	10	0	10	31	0	10
15°	38	33	18	1	0	0	0	0	12	29	37	38	38	15	0	15	35	0	14
20°	43	38	23	6	0	0	0	2	17	34	42	43	43	20	0	20	40	0	19
25°	48	43	28	11	3	2	2	7	25	38	47	48	48	26	2	25	45	3	25
30°	53	48	33	16	8	7	7	12	30	43	52	53	53	31	7	30	49	7	30
35°	58	52	38	21	13	12	12	17	35	48	57	58	58	36	12	35	54	12	35
40°	63	57	43	26	18	17	17	22	40	53	62	63	63	41	17	40	58	17	40
45°	68	62	48	31	23	22	22	27	45	58	67	68	68	46	22	45	63	22	45
50°	73	66	53	36	28	27	27	32	50	62	72	73	73	51	27	50	67	27	50
55°	78	71	58	41	33	32	32	37	55	67	77	78	78	56	32	55	71	32	55
60°	83	76	63	46	38	37	37	42	60	72	81	83	83	61	37	60	75	37	60
65°	87	80	68	51	43	42	42	47	65	76	85	88	87	66	42	65	78	42	65
70°	89	84	72	55	48	47	47	52	67	81	88	100	89	65	47	65	80	47	54
75°		87	77	60	53	52	52	57	71	85				68	52	68	82	52	56
80°		89	81	65	58	57	57	62	76	87				70	57	70	85	57	58
85°			84	70	63	62	62	67	81	90				72	62	72	88	62	62
90°			87	75	68	67	67	72	83					74	67	75		67	67

5 DISCUSSION OF THE RESULTS

As it can be seen in Table 2, the monthly (12 seasons) optimal tilting of the tropical and the mid-latitudes β_{OS} curves show the same oscillation of $\pm$ 23.45°, corresponding to the annual solar declination (δ) change. The zeros may correspond to either the optimal tilts, or to the minimal possible tilts when the panels lie on the ground and cannot tilt below, in a negative angle. In the polar latitudes, the optimal tilt can be calculated for the dates during the polar day of the Northern Hemisphere. There are no β_{OS} propositions for the polar latitudes that are entirely in the polar night. In the four-seasons model, the seasonal dates are chosen to have the least possible β_{OD} variation among the embraced days, using the graphs in Figure 5. Their β_{OS} are in accordance with the dates of all altitudes that have daylight. The same can be said for the two-seasons model. It is also obvious that fixed annual model β_{OS} for all tropical and mid-latitudes equals the corresponding latitudes, which confirms the standard engineering recommendation and practice. As expected, the polar latitudes have optimal tilting, based on the dates with daylight. The simulation results are consistent with common engineering practices, pending the experimental validation.

6 CONCLUSION

Solar energy is an abundant source of sustainable green energy, yet delicate from a harvesting perspective, due to the blocking properties of the unpredictable atmospheric conditions (vapor and particles), as well as the solar incidence angle on which the PV conversion efficiency depends.

Furthermore, the more directly (perpendicular to the sun`s rays) the PV panels are exposed, the more heated they become, which, in turn, lowers the PV conversion efficiency. Continuous automated tracking (at least for the optimal tilt, and preferably for the optimal azimuth too) is usually a significant expense, so efforts are made to maximize energy harvesting based on the optimal "seasonal" fixed tilt, with latitude being the fundamental parameter and "season" being a sequence of days with no significant change in energy conversion if the tilt is optimized daily. The problem of optimal fixed tilt calculation is recognized by the engineering community, and enormous effort is made worldwide to define such an analytical model for optimal tilting without expensive tracking or time-consuming measurements, which can be depicted in lots of published papers, like [3] - [15]. Some approaches use statistical meteorological data as a basis to determine the geometrical circumstances under which the panel had its optimal tilt for maximal efficiency. Others use regression over measured data under known weather circumstances to model the analytical expression for optimal tilt calculation, which, on the other hand, introduces some "off latitude" deviation in the results. Some of the authors consider the context's parameters, that have a significant impact on the measurements, like vapor, microparticles and pollution, which influence the local atmosphere over the panels. Interestingly, very few consider the operational heat, which lowers the PV conversion efficiency. If not addressed properly with cooling, it does coerce the model off the latitude value. Especially significant we find the work of Ogundimu @ al [14], providing a comprehensive overview of the contributions of previously published models proposing methodologies for optimal tilting at specific latitudes, providing correcting parameters that those scholars have calculated based on direct measurements or local (historical) statistical meteorological data. We believe that these approaches based on measured data or meteorological information do not always consider all circumstances influencing the resulting PV conversion efficiency, leading to those latitude corrections.

Our proposed concept for analytical estimation of the optimal PV panel tilt, based on the su`sn position and clear-sky irradiance models, provides a reliable and consistent methodology for daily tracking and arbitrary seasonal tilt optimization under ideal atmospheric conditions, as Nakamura @ al [15] support by their experimental setup. This approach is not burdened by costly and time-consuming measurements, heavy meteorological data statistics, or regression modeling. The algorithm is precise and easy to implement, thus providing an affordable and straight-forward-to-use tool for that purpose. If significant, local atmospheric conditions could be considered in the irradiance model, which would be one of the next development steps.

References

[1] **S. A. Kalogirou**: *Solar Energy Engineering Process and Systems,* Elsevier, 2009

[2] **J. A. Duffie, W. A. Beckman**: *Solar Engineering of Thermal Processes*, John Wiley and Sons, 2013

[3] **E.D. Mehleri, P.L. Zervas, H. Sarimveis, J.A. Palyvos, N.C. Markatos**: *Determination of the optimal tilt angle and orientation for solar photovoltaic arrays*, Renewable Energy, Elsevier, Vol. 35, Iss. 11, pp. 2468-2475, 2010

[4] **R. Tang, T. Wu**: *Optimal tilt-angles for solar collectors used in China*, Applied Energy, Elsevier, Vol. 79, Iss. 3, pp. 239-248, 2004

[5] **M. Yakup, A. Q. Malik**: *Optimum tilt angle and orientation for solar collector in Brunei Darussalam*, Renewable Energy, Elsevier, Vol. 24, Iss. 2, pp. 223-234, 2001

[6] **Y. B. Gebremedhen**: *Determination of Optimum Fixed and Adjustable Tilt Angles for Solar Collectors by Using Typical Meteorological Year data for Turkey*, International Journal of Renewable Energy Research, Vol. 4, Iss. 4, pp. 924-928, 2014

[7] **E. A. Handoyoa, D. Ichsania, Prabowoa**: *The optimal tilt angle of a solar collector*, International Conference on Sustainable Energy Engineering and Application 2012, Elsevier, Energy Procedia 32, pp. 166-175, 2013

[8] **A. Rouholamini, H. Pourgharibshahi, R. Fadaeinedjad, G. Moschopoulos**: *Optimal Tilt Angle Determination of Photovoltaic Panels and Comparing of their Mathematical Model Predictions to Experimental Data in Kerman*, IEEE Canadian Conference Of Electrical And Computer Engineering 2013

[9] **A. K. Abdelaal, A. El-Fergany**: *Estimation of optimal tilt angles for photovoltaic panels in Egypt with experimental verifications*, Sci Rep 13:3268, 2023

[10[**E. Gonzalez-Gonzalez, J. Martín-Jimenez, M. Saanchez-Aparicio, S. D. Pozo, S. Laguela**: *Evaluating the standards for solar PV installations in the Iberian Peninsula: Analysis of tilt angles and determination of solar climate zones*, Sustainable Energy Technologies and Assessments, Elsevier, Vol. 49, No. 101684, 2022

[11] **A. U. Obiwulu, N. Erusiafe, M. A. Olopade, S. C. Nwokolo**: *Modeling and estimation of the optimal tilt angle, maximum incident solar radiation, and global radiation index of the photovoltaic system*, Helyion, Elsevier, Vol. 8, 2022

[12] **M. A. M. Ramli, H. R. E. H. Bouchekara, M. S. Shahriar, A. H. Milyani, M. Rawa**: *Maximization of Solar Radiation on PV Panels With Optimal Intervals and Tilt Angle: Case Study of Yanbu, Saudi Arabia*, Frontiers in Energy Research, Vol. 9:753998, 2021

[13] **G. Hailu, A. S. Fung**: *Optimum Tilt Angle and Orientation of Photovoltaic Thermal System for Application in Greater Toronto Area, Canada*, Sustainability, Vol. 11, No. 22, 2019

[14] **E. O. Ogundimu, E. T. Akinlabi, C. A. Mgbemene**: *Maximizing the Output Power Harvest of a PV Panel: A Critical Review*, Journal of Physics: Conference Series, Vol. 1378, Iss. 3, 2019

[15] **H. Nakamura, T. Yamada, T. Sugiura, K. Sakuta, K. Kurokawa**: *Data analysis on solar irradiance and performance characteristics of solar modules with a test facility of various tilted angles and directions*, Solar Energy Materials & Solar Cells, Elsevier, Vol. 67, Iss. 1-4, pp. 591-600, 2001

[16] **M. Iqbal**: *An Introduction to Solar Radiation*, Academic Press Toronto, 1983

[17] **J. W. Spencer**:*Fourier series representation of the position of the sun*, Search, Vol. 2, Iss. 5, p.172, 1971

[18] **H. C. Hottel**: *A Simple Model for Estimating the Transmittance of Direct Solar Radiation through Clear Atmospheres*, Solar Energy, Vol. 18, Iss. 2, pp. 129-134, 1976

Journal of Energy Technology

JET Volume 16 (2023) p.p. 54-62
Issue 4, 2023
Type of article: 1.01
http://www.fe.um.si/si/jet.htm

SWOT ANALYSIS OF HYDROGEN ECONOMY

EKONOMIJA VODIKA S SWOT-ANALIZO

Dominik Oravec[1], Florinda F. Martins[2], Frantisek Janicek[3], Miroslava Farkas Smitkova[✉]

Keywords: Energy accumulation, energy, greenhouse gas, hydrogen, hydrogen economy

Abstract

The paper deals with the types of hydrogen production, methods for its storage and transport, and possibilities of the end use of hydrogen. The basics of the hydrogen economy are described briefly, and then the SWOT analysis is performed of the hydrogen economy. The strengths, weaknesses, opportunities, and threats of the hydrogen economy are summarized in the SWOT analysis. The biggest problems and threats, with the possibilities of solving those problems, are summarized based on that analysis. The SWOT analysis considers aspects of the hydrogen economy e.g. energy demands, financial difficulty, safety, and awareness about hydrogen. The Conclusions involve suggestions on how to avoid the above-mentioned awareness, and how to increase hydrogen utilization.

Povzetek

Prispevek obravnava vrste pridobivanja vodika, načine njegovega skladiščenja in transporta ter možnosti končne uporabe vodika. Na kratko so opisane osnove ekonomije vodika, nato pa je opravljena SWOT-analiza ekonomije vodika. Prednosti, slabosti, priložnosti in nevarnosti vodikovega gospodarstva so povzete v SWOT-analizi. Na podlagi te analize so povzeti največji

✉ Corresponding author: Assoc. Prof. Miroslava F. Smitkova, Institute of Power and Applied Electrical Engineering, Faculty of Electrical Engineering and Information Technology, Slovak University of Technology in Bratislava, Ilkovičova 3, 812 19, Bratislava, Slovak Republic Tel.: +421 2 602 91 , E-mail address: miroslava.smitkova@stuba.sk

1,3 Institute of Power and Applied Electrical Engineering, Faculty of Electrical Engineering and Information Technology, Slovak University of Technology in Bratislava, Ilkovičova 3, 812 19, Bratislava, Slovak Republic

2 School of Engineering (Instituto Superior de Engenharia do Porto), Polytechnic of Porto (P.Porto), Porto, Portugal

problemi in nevarnosti z možnostmi reševanja teh problemov. SWOT-analiza upošteva vidike vodikovega gospodarstva, npr. energetske zahteve, finančne težave, varnost in ozaveščenost o vodiku. Sklepi vključujejo predloge, kako se izogniti zgoraj omenjenemu zavedanju in kako povečati izkoristek vodika.

1 INTRODUCTION

Nowadays, industrially developed countries are using energy mainly from fossil fuels, which are not infinite resources. That is causing faster development in energy resources and possibilities of accumulation energy. The main alternative sources are renewable energy resources with low negative impact on the environment. Renewable resources are difficult to predict in terms of production. This causes the necessity to accumulate energy during high energy production. Current ways for energy accumulation are, e.g., pumped-storage hydroelectricity or batteries. Hydrogen represents another way to accumulate energy. The hydrogen economy deals with issues around the accumulation of energy in hydrogen form, e.g. from renewable sources or fossil fuels. There is an effort to find the best ways for the production, storage, transport, and end use of hydrogen.

2 HYDROGEN PRODUCTION

Production of hydrogen is a process where there is a splitting chemical bond of water which produces separated hydrogen and oxygen. We divide the hydrogen in the color spectrum. Every color depends on the method of production, see Table 1. Each color corresponds to a different extraction process. Nevertheless, the steam reforming of fossil fuels creates the most greenhouse gases. It is the most used method of hydrogen production. Selected methods of hydrogen production are described in Table 2.

Table 1: *Color marking of hydrogen*

Color	Method of production
Gray hydrogen	Hydrogen is produced by the steam reforming of fossil fuels. Nowadays, it is the most used method of hydrogen production. This method doesn't use capture devices.
Brown/Black hydrogen	The process of hydrogen production is using black or brown coal. It has the worst impact on the environment.
Blue hydrogen	Hydrogen is produced by the steam reforming of fossil fuels with capture devices. The reduction of greenhouse gases is around 90 %.
Pink hydrogen	Hydrogen is produced through electrolysis, using a high temperature from nuclear reactors. It can also be referred to as red or purple hydrogen.
Turquoise hydrogen	A process called methane pyrolysis is used. In the future, it may be valued as a low-emission hydrogen. It depends if the process is powered by renewable sources.
Yellow hydrogen	It is a new phase. The electrolysis uses solar energy.
White hydrogen	Geological hydrogen is found in underground deposits and created by fracking. There is no strategy for how to use this hydrogen.
Green hydrogen	The energy for electrolysis comes from renewable sources like photovoltaic panels or wind turbines.

Table 2: *Hydrogen production method*

Method of production	Brief description of production
Electrolysis	The chemical bond of water is split by an electric current.
Thermochemical cycles	An endothermic process where energy from nuclear or solar sources is used for the thermal splitting of water.
Steam reforming of natural gas	The endothermic reaction of natural gas and water vapor. Water vapor has a temperature around 750 – 900 °C. This process creates hydrogen, carbon monoxide, and a smaller amount of carbon dioxide.

Nowadays, mainly fossil fuels are used for hydrogen production, which amount is around 96% of the total production. Electrolysis of water covers the rest, just 4%, see Figure 1.

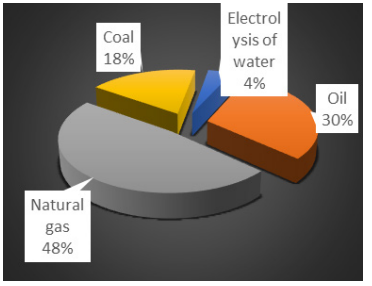

Figure 1: *Division of hydrogen production*

3 HYDROGEN STORAGE

Hydrogen can be stored in different forms, and every form has specific energy demands. Options for storage are hydrogen in gas form, liquid hydrogen and hydrids, where the hydrogen is bound to different alloys.

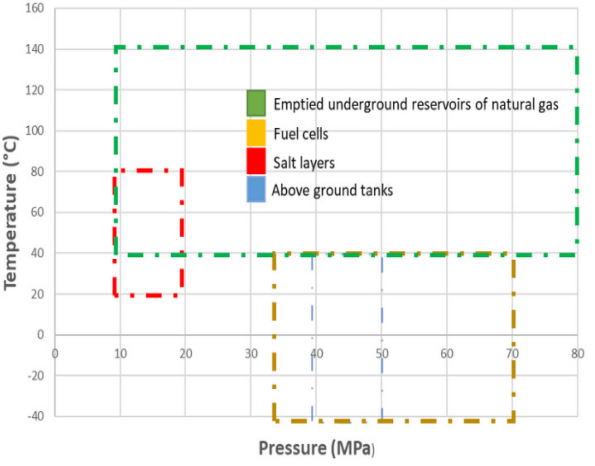

Figure 2: *Division of hydrogen production*

3.1 Storage of hydrogen in gas form

For industry and large-capacity hydrogen storage, it is convenient to store hydrogen in a gas form. In gas form hydrogen can be stored in pressure vessels above the ground or undersea. For large-capacity hydrogen storage emptied underground reservoirs of natural gas or salt layers are the most advantageous. Every method for hydrogen storage requires different temperatures and pressures, see Figure 2. In this method of storage, energy losses are caused by compression devices for compressing hydrogen, or, in the case of underground reservoirs, some of the hydrogen settles in the micropores of the soil.

3.2 Storage of hydrogen in liquid form

In the development of storage hydrogen in liquid form the NASA organization has a major share, where liquid hydrogen is used as rocket fuel. Liquefaction is an energy demanding process where the hydrogen must be cooled at a temperature around -253 °C. This process consumes 15,1 MJ/kg energy *[1]*. The energy needs for hydrogen storage in a liquid form are affected by gas purity, because it is necessary to separate other gases (expected helium) from the hydrogen. Mainly oxygen separation is very important, because the concentration of more than 1 mg of oxygen on 1 kg of hydrogen causes an explosion *[1]*. Other energy losses are caused by the transition of hydrogen from orthoform to paraform. Orthoform has symmetric spins of atoms, and in the paraform, these spins are not symmetric. Para-hydrogen is more stable at lower temperatures, and has a lower enthalpy capacity. Therefore, when hydrogen is passing from orthoform to paraform, the heat is released, which increases the energy requirement.

3.3 Storage of hydrogen in a hydrid form

Storage reservoirs in the case of the hydrid form are smaller than other forms. This type of storage is suitable for end consumers. Hydrogen is bound to other energy carriers, like metal and metal alloys, which creates metal hydrids. For every metal alloy it is required to find the right temperature and pressure when the hydrogen is bound to the metal. It is an exothermic reaction, where, during the fulfilment of the reservoir heat is released and it is necessary for the reservoir to cool down, because this can cause the release of hydrogen. To release hydrogen from the reservoir, the reservoir must be heated or depressurized.

4 HYDROGEN TRANSPORT

Hydrogen can be transported in gaseous, as well as liquid form. For longer distances hydrogen can be distributed through long-distance gas pipelines, which are developed in every economically advanced country. For transport over shorter and medium distances, up to approximately 500 km, it is economically advantageous to transport the hydrogen in liquid or hydrid form.

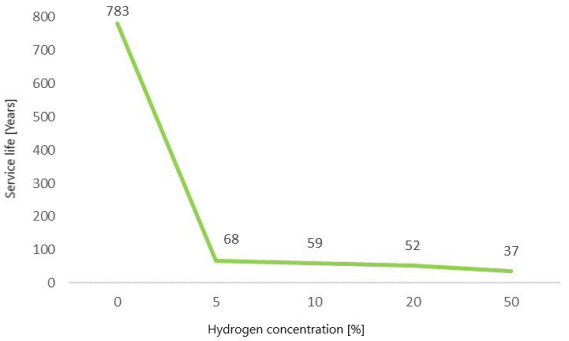

Figure 3: *Effect of bigger hydrogen concentration on the service life of the currently used pipelines*

4.1 Transport of hydrogen in gas form

To transfer the same amount of energy it is necessary to transport a three times bigger amount of hydrogen compared to natural gas, because hydrogen has a smaller heat value *[1]*. Hydrogen has a nine times smaller density than natural gas, so we can transport more hydrogen. The problem occurs at pressures higher than 5.6 MPa, when the heat value of natural gas increases and hydrogen cannot compete with natural gas. *[1]* Choosing the right gas flow, a turbulent flow, we can ensure the transport of up to 280% of the volume of hydrogen compared to natural gas, which represents approximately 95% of the energy equivalent. *[1]* The next problem of hydrogen transport in gas form is hydrogen embrittlement, where particles of the hydrogen penetrate to the material structure and cause hydrogen embrittlement. The larger amounts of pressures and concentration of hydrogen cause faster hydrogen embrittlement. It is an undesirable phenomenon which causes bigger financial investments. In Figure 3, we can see how the hydrogen concentration affects the service life of steel material. *[7]*

4.2 Transport of hydrogen in liquid form

Despite energy losses, hydrogen transport in liquid form is preferable, mainly over short distances, see Figure 4.

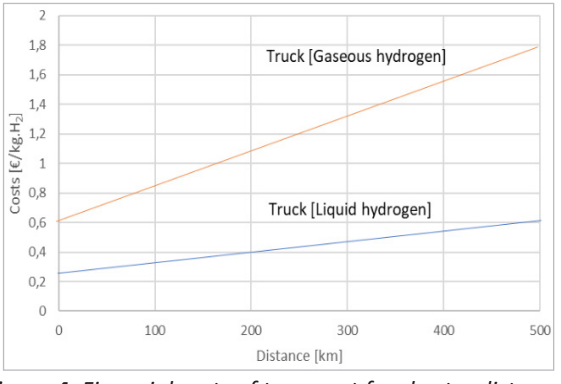

Figure 4: *Financial costs of transport for shorter distances*

Economically, costs for gaseous transport are affected by the demand for 3 times more hydrogen than natural gas. For comparison, the financial costs of different ways of hydrogen transport are shown in Table 3.

Table 3: *The comparison size of hydrogen containers. The calculated volume is needed for the storage amount of energy of 1 kWh.*

Method of storage	Density [kg/m^2]	Energetic density [MJ/m^3]	Energetic density [kWh/m^3]	Volume [m^3]	Volume [l]
Gaseous hydrogen	0.09	10	2.78	0.36	359.712
Gaseous hydrogen under a pressure of 30 MPa	22.5	2 700	750	0.0013	1.33
Liquid hydrogen	71.9	8 700	2 416.67	0.000414	0.41
Natural gas	0.668	37.4	10.39	0.096	96.25
Methanol	0.79	17 000	4 722.22	0.000212	0.21

5 USES OF HYDROGEN

The use of hydrogen in power engineering and as fuel should help the transition to a less environmentally harmful way of producing electricity, heat, or fuel. Hydrogen is deemed to be a prospective secondary energy source. Its application is universal – e.g. power engineering (electricity and heat production), transport, metallurgy, synthetic fertilizer production, usage in the oil industry.

5.1 Uses in power engineering

Hydrogen can help in the decarbonization of electricity production. Green hydrogen can potentially store 4 – 20% of energy from renewable sources. These percentages can increase with an increasing number of renewable sources. *[4]*

We can use hydrogen in thermomechanical cycles via the Carnot turbine, because, when hydrogen is burned with oxygen, it does not produce CO_2. If we burn hydrogen with air, it will have 1.88 mol of nitrogen that decreases part of the thermal energy *[1]*. During the burning of hydrogen with air, we do not achieve the same combustion temperature as in combustion with oxygen, so the whole process of accumulation of energy has lower efficiency.

Hydrogen has a higher flame temperature (2400 K) than natural gas, so it can be good for heat production *[1].* Also, lower energy is required for lighting the flame. Higher temperatures need appropriate technologies that can resist heat. Because 3 times more hydrogen than natural gas is needed to transfer the same amount of energy, hydrogen is currently only blended into gas pipelines. However, it is an opportunity to decarbonize the heating industry in the future.

One of the remarkable methods for large-scale hydrogen production is a thermochemical water decomposition using heat energy from nuclear, solar, and other sources. Water splitting thermochemical cycles replace the thermal decomposition of water with several partial reactions, and they represent an environmentally attractive way for hydrogen production without using fossil fuels. Hydrogen produced via the mentioned cycles could be used for electricity and heat production, as well as a fuel.

5.2 Uses in fuel cells

Fuel cells are electrochemical systems in which the chemical energy of the fuel is converted to electrical energy through the oxidation process. Losses in this system are caused by low-potential heat. The efficiency of this system depends on the activation overvoltage of the electrodes, ohmic and concentration overvoltage.

Fuel cells have better efficiency up to a temperature of 800 °C *[8].* With increasing temperature the equilibrium oxygen-hydrogen tension decreases, and, from a thermodynamic point of view, the efficiency also decreases. There are several types of fuel cells, which differ in functional principle and suitability for use. Nowadays, fuel cells do not represent an adequate large-capacity source. Fuel cells are applied in a direct current source for electric motors in cars. Fuel cells are used mainly in the automotive and aerospace industries. Fuel cells are, for example, a source of energy for space shuttles, and they were also used in the Apollo program. They are also used in submarines. Currently, some automobile manufacturers produce cars that run on hydrogen, and there are also buses which use hydrogen as a fuel. With the expansion of this type of cars, the network of hydrogen filling stations is expanding, for example, in Slovakia, the first hydrogen filling station was put into operation in 2022. Most hydrogen stations are in Japan (almost 150) and Germany (almost 100).

6 SWOT ANALYISIS

SWOT analysis is a comprehensive assessment of internal and external factors. Th strengths of SWOT analysis are simplicity, clarity, and complexity. In the internal analysis we compare S (strengths) and W (weaknesses). Parts of the external analysis are O (opportunities) and T (threats).

Table 4: *Criteria of SWOT analysis*

	S – Strengths		W – Weaknesses		O – Opportunities		T – Threats
S1	Accumulation method that doesn't have a negative impact on the environment – depends on the production method	W1	Hydrogen, due to its properties and high diffusion, causes hydrogen embrittlement of the material	O1	Creation of new job opportunities – it is a new technology that requires new, professionally educated people	T1	New technology – the possibility of higher danger
S2	Use of renewable sources in production – electrolysis of water, thermochemical cycles	W2	Requiring a 3 times more amount of hydrogen to transfer the same amount of energy as natural gas, due to lower calorific value	O2	Energy independence – reduced dependence on imports	T2	High investment, need for staff training, developing new technologies etc.
S3	Slowdown in the decline of the Earth's fossil fuel reserves (oil, natural gas)	W3	High financial costs of hydrogen production	O3	Reduction of environmental pollution – depending on the production method (green hydrogen)	T3	Currently underdeveloped infrastructure

S4	A new energy carrier – less dependence on fossil fuels	W4	Energetic intensity of storage – liquefaction, gas compression	O4	Opportunity to use old depleted underground natural gas reservoirs	T4	Competition from cheaper energy sources (fossil fuels)
S5	Building new refuelling stations for a hydrogen economy	W5	Low efficiency of fuel cells, need to provide new technology to increase efficiency	O5	Reducing commodity price fluctuations	T5	Lack of information delivered to the public

The result of the contribution is a SWOT analysis of the hydrogen economy. The criteria used in the SWOT analysis are shown in Table 4. In Table 5 there is a comparison matrix, from which we get specific results about strengths, weaknesses, opportunities, and threats. In Table 5, scoring is used on a scale of minus 5 to plus 5, where minus 5 represents the worst negative mutual influence and 5 represents the best positive mutual influence.

Table 5: *Comparison matrix*

		Internal factors											
		S – Strengths						W - Weaknesses					
Key external factors	O - Opportunities T – Threats	S1	S2	S3	S4	S5	The sum of the ratings O,T/S	W1	W2	W3	W4	W5	The sum of the ratings O,T/W	Final evaluation
	O1	0	5	3	5	5	18	4	2	-2	3	3	10	28
	O2	2	5	3	5	3	18	2	3	3	5	4	17	35
	O3	5	5	3	3	3	19	3	2	4	3	3	15	34
	O4	3	0	-4	2	1	2	1	4	3	1	0	9	11
	O5	1	3	2	5	1	12	3	1	5	4	4	17	29
	T1	0	-2	-4	-4	-2	-12	-5	-3	0	-4	0	-12	-24
	T2	-1	-2	-4	-5	-3	-15	-3	-2	-5	-3	-5	-18	-33
	T3	0	-1	-2	-3	-5	-11	-1	-3	-5	0	-3	-12	-23
	T4	-5	-5	-5	-5	-5	-25	-4	-5	-4	-4	-3	-20	-45
	T5	-5	0	-2	-2	-1	-10	-3	2	-3	0	-3	-7	-17
The sum of the ratings S,W		0	8	-10	1	-3	-4	-3	1	-4	5	0	-1	-5
Scale S / W		35	25	15	15	10	/	15	25	20	30	10		

7 CONCLUSIONS

From the SWOT analysis we found out that the most prominent strength is S2 – Using renewable sources, immediately followed by S1 – the Accumulation method without a negative impact on the environment. In the strategy we should focus on these strengths, and ensure that T4 and T5 will be reduced. T4 – Competition from cheaper energy sources, can be countered by increasing renewable sources that will be used for hydrogen production, or possibly thermochemical cycles. T5 – Lack of information delivered to the public, can be countered by lectures, various discussions, articles, and general propagation. The biggest weaknesses are W2 – Requiring a bigger amount of hydrogen than natural gas, and W4 – The energetic intensity of storage. W2 is related to the opportunity of O4 – the Opportunity to use old depleted natural gas reservoirs. These depleted natural gas reservoirs are good for high-capacity storage. Storage of hydrogen is an energetic challenge, because there are big energy losses. When hydrogen is compressed to 350 bars, approximately 15 – 20% of the energy contained in the fuel is required for the function of compressors, measuring devices, etc. Hydrogen in liquid form has bigger losses, approximately 30 – 40% of energy contained in the fuel is needed for liquefaction. Despite the higher energy intensity of storage, some opportunities have positive impacts, like O2 – Energy independence, and O5 - Reducing commodity price fluctuations.

Acknowledgements

This work was supported by the Slovak Research and Development Agency under the Contract No. APVV-20-0157".

References

[1] **J. Balajka:** *Vodík a iné nosiče energie*, ALFA, 1982

[2] **G. Franchi. et al.:** *Hydrogen production via steam reforming: a critical analysis of MR and RMM technologies*, PubMed, 2022

[3] **Hassanpouryouzband, A. *et al*.,** *Thermodynamic and transport properties of hydrogen containing streams*, Scientific Data, 2020

[4] *Národná vodíková asociácia*, [online], 2022, Available: nvas.sk (4.5.2023)

[5] *NATIONALGRID - The hydrogen colour spectrum,* [online], 2022, Available: www.nationalgrid.com/stories/energy-explained/hydrogen-colour-spectrum (7.4.2023)

[6] **M.J. Ogden**, *Hydrogen Infrastructure Capital Costs Compared with Those for Methanol, Gasoline, and Synthetic Middle Distillates*, Researchgate, p.p. 262, 2020

[7] **V. Olej**, *Úskalia prepravy vodíka plynárenskou infraštruktúrou*, Slovgas: 2020

[8] **B. Petráš, T. Brestovič,** *Palivový článok – zdroj energie*, AT&P journal: Technická univerzita Košice, Strojnícka fakulta, 2007

[9] **C. Vargas-Salgado, et al**., *Hydrogen Production from Surplus Electricity Generated by an Autonomous Renewable System*. Scenario 2040 on Grand Canary Island, Spain, p.p.12, 2022

Journal of Energy Technology

Author instructions

http://www.fe.um.si/si/jet.htm

MAIN TITLE OF THE PAPER

SLOVENIAN TITLE

Author[1], Author [2], Corresponding author [ℜ]

Keywords: (Up to 10 keywords)

Abstract

Abstract should be up to 500 words long, with no pictures, photos, equations, tables, only text.

Povzetek

(Abstract in Slovenian language)

Submission of Manuscripts: All manuscripts must be submitted in English by e-mail to the editorial office at jet@um.si to ensure fast processing. Instructions for authors are also available online at http://www.fe.um.si/en/jet/author-instructions.html.

Preparation of manuscripts: Manuscripts must be typed in English in prescribed journal form (MS Word editor). A MS Word template is available at the Journal Home page.

A title page consists of the main title in the English and Slovenian language; the author(s) name(s) as well as the address, affiliation, E-mail address, telephone and fax numbers of author(s). Corresponding author must be indicated.

Main title: should be centred and written with capital letters (ARIAL bold 18 pt), in first paragraph in English language, in second paragraph in Slovenian language.

Key words: A list of 3 up to 6 key words is essential for indexing purposes. (CALIBRI 10pt)

[ℜ] Corresponding author: Title, Name and Surname, Organisation, Department, Address, Tel.: +XXX x xxx xxx, E-mail address: x.x@xxx.xx

[1] Organisation, Department, Address

[2] Organisation, Department, Address

Abstract: Abstract should be up to 500 words long, with no pictures, photos, equations, tables, - text only.

Povzetek: - Abstract in Slovenian language.

Main text should be structured logically in chapters, sections and sub-sections. Type of letters is Calibri, 10pt, full justified.

Units and abbreviations: Required are SI units. Abbreviations must be given in text when first mentioned.

Proofreading: The proof will be send by e-mail to the corresponding author in MS Word's Track changes function. Corresponding author is required to make their proof corrections with accepting or rejecting the tracked changes in document and answer all open comments of proof reader. The corresponding author is responsible to introduce corrections of data in the paper. The Editors are not responsible for damage or loss of submitted text. Contributors are advised to keep copies of their texts, illustrations and all other materials.

The statements, opinions and data contained in this publication are solely those of the individual authors and not of the publisher and the Editors. Neither the publisher nor the Editors can accept any legal responsibility for errors that could appear during the process.

Chapter examples:

1 MAIN CHAPTER (Arial bold, 12pt, after paragraph 6pt space)

1.1 Section (Arial bold, 11pt, after paragraph 6pt space)

1.1.1 Sub-section (Arial bold, 10pt, after paragraph 6pt space)

Example of Equation (lined 2 cm from left margin, equation number in normal brackets (section.equation number), lined right margin, paragraph space 6pt before in after line):

Equation (1.1)

Tables should have a legend that includes the title of the table at the top of the table. Each table should be cited in the text.

Table legend example:

Table 1: *Name of the table (centred, on top of the table)*

Figures and images should be labelled sequentially numbered (Arabic numbers) and cited in the text – Fig.1 or Figure 1. The legend should be below the image, picture, photo or drawing.

Figure legend example:

Figure 1: *Name of the figure (centred, on bottom of figure, photo, or drawing)*

References

[1] **N. Surname:** *Title,* Journal Title, Vol., Iss., p.p., Year of Publication

[2] **N. Surname:** *Title,* Publisher, Year of Publication

[3] **N. Surname:** *Title* [online], Publisher or Journal Title, Vol., Iss., p.p., Year of Publication. Available: website (date accessed)

Examples:

[1] **J. Usenik**: *Mathematical model of the power supply system control*, Journal of Energy Technology, Vol. 2, Iss. 3, p.p. 29 – 46, 2009

[2] **J. J. DiStefano, A.R. Stubberud, I. J. Williams**: *Theory and Problems of Feedback and Control Systems*, McGraw-Hill Book Company, 1987

[3] **T. Žagar, L. Kegel**: *Preparation of National programme for SF and RW management taking into account the possible future evolution of ERDO* [online], Journal of Energy Technology, Vol. 9, Iss. 1, p.p. 39 – 50, 2016. Available: http://www.fe.um.si/images/jet/Volume 9_Issue1/03-JET_marec_2016-PREPARATION_OF_NATIONAL.pdf (7. 10. 2016)

Example of reference-1 citation: In text *[1],* text continue.

Nomenclature

(Symbols)	(Symbol meaning)
t	time

JET I Journal of Energy Technology I Vol. 16, Issue 4, December 2023 I University of Maribor, Faculty of Energy Technology

ISSN 1855-5748

9 771855 574008